Aalborg Universitet

AALBORG UNIVERSITY
DENMARK

Combining weather radar nowcasts and numerical weather prediction models to estimate short-term quantitative precipitation and uncertainty
Jensen, David Getreuer

COMBINING WEATHER RADAR NOWCASTS AND NUMERICAL WEATHER PREDICTION MODELS TO ESTIMATE SHORT-TERM QUANTITATIVE PRECIPITATION AND UNCERTAINTY

BY
DAVID GETREUER JENSEN

DISSERTATION SUBMITTED 2015

AALBORG UNIVERSITY
DENMARK

COMBINING WEATHER RADAR NOWCASTS AND NUMERICAL WEATHER PREDICTION MODELS TO ESTIMATE SHORT-TERM QUANTITATIVE PRECIPITATION AND UNCERTAINTY

by

David Getreuer Jensen

AALBORG UNIVERSITY
DENMARK

Dissertation submitted

.

PREFACE

This thesis is prepared as a part of a Ph.D. study during the period November 1, 2012 to October 15 2015 at the Department of Civil Engineering, Aalborg University, Denmark. The Ph.D. study is funded by the Strategic Research in Sustainable Energy and Environment and is part of HydroCast – Hydrological forecasting and data assimilation project. The study is supervised by Associate Professor Michael Robdrup Rasmussen and conducted in cooperation with the Danish Meteorological Institute (DMI). The thesis consists of five journal papers and one technical note as well as an introductive review and summery.

First of all, I would like to thank my supervisor Michael Robdrup Rasmussen for many good talks, support, loyalty and guidance throughout the study. I would also like to thank Jesper E. Nielsen for the many professional as well as personal talks. Furthermore I would like to express my gratitude to Søren Thorndahl for valuable discussions and inputs to the project. Lastly, a thanks to the Department for making it a nice place to work.

I would also like to thank Centre for Meteorological Models, Research and Development Department at DMI for the very fruitful research stays. A special thanks goes to Claus Petersen, for the good talks and great help with the study.

Another thanks goes to Kevin Martin for his excellent work of proof reading.

Special thanks to my wife Sanne for her love and support throughout the project.

Aalborg, October 2015

David Getreuer Jensen

ENGLISH SUMMARY

The topic of this Ph.D. thesis is short term forecasting of precipitation for up to 6 hours called nowcasts. The focus is on improving the precision of deterministic nowcasts, assimilation of radar extrapolation model (REM) data into Danish Meteorological Institutes (DMI) HIRLAM numerical weather prediction (NWP) model and produce quantitative estimations of nowcast uncertainty.

In real time control of urban drainage systems, nowcasting is used to increase the margin for decision-making. The spatial extent of urban drainage catchments is very small in a meteorological context. This is a problem since small scale features of the precipitation are the least predictable and hence very difficult to anticipate. This also leads to uncertainty at urban scale, which needs to be addressed.

Initially, Kalman filtering is used to stabilise the advection field in order to increase the precision of a Co-TREC based REM. The filter is calibrated against atmospheric observations of radial velocity measured by a Doppler radar. The results from pooled skill scores from 16 events show only a slight improvement. The positive contribution, from applying Kalman filtering, is increased stability computed by the relative standard deviation.

A significant result of this Ph.D. study is major improvements in predictability of DMI HIRLAM NWP model by assimilation of REM data. A new nudging assimilation method developed at DMI was used to assimilate the REM data. The assimilation technique enhances convection in case of under-prediction of precipitation and reduces convection in the opposite case. The result is based on evaluation of 8 events from august 2010 and an extreme event from 2 July 2011. Both spatial predictability and accumulated volumes benefit from the REM data assimilation. The system is currently being tested at DMI to become an operational system.

To address the uncertainty of REM nowcasting, a new ensemble prediction system was developed called RESEMBLE (Rainfall Extrapolation System – EnseMBLE). The novelty of this method is the separation of advection – and evolution uncertainty and the way the temporal correlation is incorporated by a numerical interpolation technique. The results demonstrate that ensemble mean performs with higher correlation than the deterministic prediction compared to observations. The system, with good skill, is able to predict the location and intensity of precipitation and the ensemble spread is in proportion to the uncertainty of ensemble mean. The system is also tested as input for an urban drainage system with promising results.

The encouraging results from assimilation of REM data into DMI HIRLAM NWP model also inspired the work of initiating HIRLAM NWP ensemble members by

assimilation of REM ensemble members. The same nudging assimilation technique was applied to assimilate ensemble members from RESEMBLE into the NWP model. The results showed a rapid initiation of ensemble members, reasonable reproduction of nowcast uncertainty and a higher performance than ensemble mean than runs without using RESEMBLE assimilation. A slight bias was also demonstrated in the prediction towards high intensities but this was expected since the model was tuned towards high intensity precipitation.

DANSK RESUME

Temaet for indeværende Ph.D. afhandling er forudsigelse af nedbør op til 6 timer frem i tiden også kaldet nowcasts. Der er fokus på at forbedre præcisionen af deterministiske nowcasts, assimilering af radar ekstrapolations modeller (REM) i Dansk Meteorologisk Instituts (DMI) HIRLAM numeriske vejrmodel (NWP), samt kvantificering af nowcast usikkerhed.

Indenfor realtidsstyring af afløbssystemer bliver nowcasts brugt til at udvide den margin der er til at træffe styringsbeslutninger i forhold til kun at anvende observationer. Den spatial udstrækning af afløbssystemer er lille i forhold til meteorologiske skala. Dette udgør et problem i forhold til at kunne forudsige nedbøren eftersom de små skalaer også er dem der har kortest levetid og herved er de sværeste at forudsige. Ydermere betyder det også at der er stor usikkerhed ved forudsigelser på afløbsteknisk skala. Dette er motivationen for at arbejde med at forbedre forudsigelsen af nedbør.

For at forbedre præcisionen af REM nowcasts er et Kalman filter implementeret for at stabilisere flytningsfeltet. Filteret er kalibreret op mod radar-Doppler målinger af den atmosfæriske ændring i radial hastighed af nedbøren. Implementeringen af Kalman filteret blev igennem pooled skill scores evalueret for 16 hændelser. Resultatet viste kun en lille tendens til forbedring af forudsigelserne. Den egentligt fordel ved implementeringen er en stabilisering af præstationsniveauet hvilket er bekræftet vha. beregning af den relative standard afvigelse.

Et meget signifikant resultat for denne Ph.D. er opnået ved assimilering af REM data i DMI HIRLAM NWP model. Assimileringen blev foretaget vha. en nudging metode, udviklet på DMI, der forstærker konvektion når der underestimeres og reducere når der overestimeres. Metoden blev evalueret for 8 hændelser fra august 2010 samt en ekstrem hændelse d. 2 juli 2011. Resultaterne viser en væsentlig forbedring i både den spatiale forudsigelse og i akkumulerede nedbørsmængder. Systemet er for nuværende i gang med at blive testet ved DMI med henblik på at fungere operationelt.

For at adressere usikkerhed i REM forudsigelser er et nyt ensemble forudsigelses system udviklet. Metoden kaldes RESEMBLE (Rainfall Extrapolation System – EnseMBLE). Det der gør denne model anderledes, end andre systemer, er måden hvorpå usikkerheden er opdelt og behandlet i dens komponenter – advektionsusikkerhed samt evolutionsusikkerhed. Ydermere er den temporale korrelation estimeret vha. en numerisk interpolations metode. Resultaterne viser at gennemsnits ensemblet har højere korrelation med observationer end den deterministiske forudsigelse, samt at RESEMBLE er i stand til at forudsige lokaliteten af regnen. Yderligere viste evalueringen at spredningen på ensemblerne

er i overensstemmelse med nowcast-usikkerheden. RESEMBLE blev også testet som input i en afløbsmodel. Resultaterne virker lovende.

De gode resultater ved assimilering af REM data i DMI HIRLAM NWP model inspirerede til at initiere NWP ensembler ved at assimilere RESEMBLE ensembler. Dette blev gjort ved at benytte samme assimileringsteknik som blev anvendt i tidligere forsøg. Resultat viste en hurtig initiering af NWP ensembler, en fornuftig reproduktion af nowcast-usikkerheden og et bedre præstationsniveau af gennemsnit ensemblet i forhold til kørsler uden assimilering af RESEMBLE. En bias mod højere intensiteter blev også fundet. Dette var dog forventet siden assimileringen var tunet mod at forudsige høje intensiteter.

TABLE OF CONTENT

CHAPTER 1. INTRODUCTION

The precipitation pattern over Denmark will, in the future, change due to climate changes. According to Pachauri, Allen et al. (2014), it is *very likely* that the precipitation will become more frequent and intense as global mean temperature increases. Furthermore, as urbanisation is increasing, more impervious areas are contributing to an increased amount of water in the drainage system. The combination of higher precipitation intensity and urbanisation results in further stress on the cities drainage systems. These factors also contributed to a significant increase in economic loss from flooding since the 1950's (Christensen, Arnbjerg-Nielsen et al. 2014). Pachauri, Allen et al. (2014) also states, with *very high* confidence that the tendency of increased frequency of urban floods will continue.

Urban floods due to heavy precipitation can be extremely costly for the society. As a recent example, a flood of the Copenhagen area on the 2nd July 2011 costed approximately 6bn Danish DKK in damage costs (Krawack, Madsen 2013), see Figure 1.
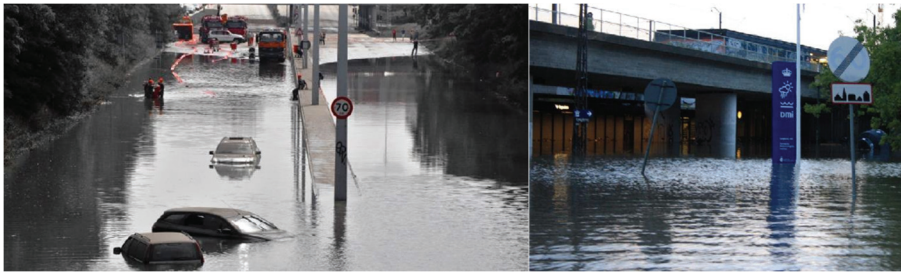
Figure 1: Flooding of Copenhagen 2nd July 2011. Image to the left taken by Per Folkver and the image to the right by Finn Majlergaard.

Adaptation of the drainage system can be done by physically upgrading the capacity. This is achieved by enlarging pipe dimensions and basin volumes but is very costly and, in some places, problematic due to urban development. For these reasons, a new tendency is seen to move towards more dynamically controlled systems, or real time control (RTC), in order to increase capacity.

RTC of the drainage system has the purpose of increasing the existing system capacity in order to minimise urban floods and minimise combined sewer overflow (CSO). RTC is to intelligently control pumps and valves within the drainage system to reroute water to areas where it will cause less damage or less precipitation is expected. Doing so releases capacity in the remaining drainage system. The control is typically based on sensors within the system and simulated water levels through

distributed urban rainfall-runoff models combined with pipe flow sub models. For extreme events, such as 2nd July 2011, flooding is unavoidable even with the application of RTC due to the large volume of water. However, with proper RTC, the damages and costs could most likely have been minimised.

The driving input for RTC of drainage systems is the precipitation. Often, ground observations and more recently also radar quantitative precipitation estimates (QPE) are used as inputs. Radar QPE has the advantage of high spatiotemporal resolution and large coverage compared to point measurements. Research has shown that radar QPE improves the simulated response for small to medium sized urban catchments (Pfister, Cassar 1999, Sempere-Torres, Corral et al. 1999, Ogden, Sharif et al. 2000, Gourley, Giangrande et al. 2010, Löwe, Thorndahl et al. 2014).

Radar QPE is not only used as an observation but also to generate short term forecasts (up to 6 hours in advance) called nowcasts. The nowcast is generated by extrapolation of the current precipitation field according to an estimated motion field. Nowcasts can provide knowledge of where and how much precipitation will fall in the future within the urban catchment. The advantage is that it enlarges the margin for decisions making (Krämer, Fuchs et al. 2007) which can be crucial for correct RTC. Several studies have shown that there is a considerable benefit for RTC in using future predictions of precipitation compared to the alternative of not using future predictions (Vivoni, Entekhabi et al. 2007, Krämer, Fuchs et al. 2007, Werner, Cranston 2009). However, urban drainage operates on small spatial scales, which is also the least predictable (Venugopal, Foufoula-Georgiou et al. 1999, Germann, Zawadzki 2002, Seed 2003).

Since the predictability of the precipitation exhibits scale dependencies with short lifetimes for small scales and urban scales, it is difficult to correctly predict these small scale features of the precipitation. As a consequence it is only possible to produce nowcasts with very short lead-times. The uncertainty will, as a function of lead time, rapidly increase to a point where skill is lost and the nowcasts can no longer be applied for RTC. For RTC, it is just as important to know the uncertainty of a prediction as the prediction itself. Low intensities could lead the operator to a false sense of safety if the uncertainty is high at the same time. On the other hand, if the prediction is high intensity with high uncertainty then the lack of information could potentially lead to a poor decision, which may cause more harm than good. There is therefore a need to increase the skill on longer lead-times of nowcasts and to quantify the uncertainty.

In order to address this problem, the work of the Ph.D. thesis is divided into three focus areas. The first focus area is to improve the spatial precision of nowcasts based on extrapolation of radar QPE (hereafter REM for radar extrapolation model). The second focus area is to combine REM with a numerical weather prediction (NWP) model, by assimilation, to improve predictability on longer lead-times. The

third focus area is to quantify and describe the uncertainty of nowcasts. These focus areas set the framework for the current Ph.D. study.

1.1. HOW TO PREDICT PRECIPITATION

There are two principal methods to generate nowcasts that are able to predict the location and intensity of precipitation. The first method is a radar extrapolation model (REM) prediction and the second is a numerical weather prediction (NWP) model prediction. The two methodologies have some similarities but are fundamentally very different.

REM is, as the name implies, an extrapolation of the current observed precipitation field measured by radar. The concept of REM is fairly simple. It consists of two major components. These are 1) Estimating the motion of the precipitation field and 2) Extrapolating the precipitation field into the future according to the estimated motion. The strengths of REM are a short computational time, high spatial and temporal resolution and high performance for very short lead-times. However, the disadvantage is that the quality of the nowcast very rapidly deteriorates since the predicted precipitation field is merely an extrapolation of the current precipitation field and does not include meteorological processes.

NWP models are not just an extrapolation of the current precipitation field but a numerical interpretation of the atmospheric state coupled with physical processes. Numerical models need both boundary conditions and initial conditions to run the simulation. In a Danish context, the boundary conditions are obtained from a model of the northern hemisphere provided by the European Centre for Medium range Weather Forecast (ECMWF). The boundary conditions are used to simulate the boundary conditions for an even smaller nested model with increasing precision. This is repeated until the desired model area and precision are obtained. The initial conditions are estimated from a vast amount of observations and are assimilated into the models at all nested levels. Observations come from numerous weather stations, different satellites, weather radars, weather balloons, aircrafts, ships, buoys and more. The advantage of NWP models is that the quality of the prediction is more persistent than REM predictions due to the description of the evolution and decay of the precipitation. The NWP model actually predicts the future state of the earth's atmosphere and therefore also models how it evolves. The disadvantages are a longer computational time, the need for a vast amount of observations and often also a more coarse spatial and temporal resolution due to the computational demands.

The above mentioned strength and weaknesses of the two methodologies affects the quality of the forecast which is conceptualised in Figure 2.

REM prediction at
urban scale

REM prediction at
continental scale

NWP model at
urban scale

REM assimilated
NWP model at
urban scale

Synoptic-scale NWP model
with model output statistics

Quality of forecast

6   12   18   24   30   36

Lead-time of forecast [hr]
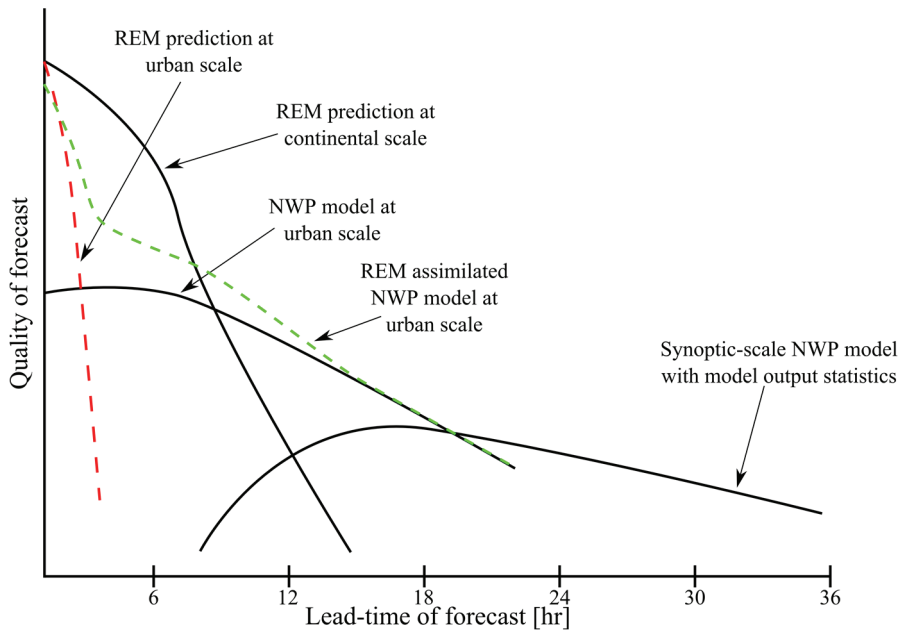
Figure 2: Solid lines: Conceptualisation of the relationship between forecasting methodology, skill and forecast range. Schematic diagram after Browning (1980). The red and green stippled line is added to the diagram to conceptualise REM quality on urban scales and the quality of REM assimilated into NWP model, respectively.

The conceptualised idea of quality, from 1980, has been shown by Bowler, Pierce et al. (2006) and Berenguer, Surcel et al. (2012) to still be valid. The quality of the extrapolation model at a continental scale is higher, for lead-times up to 8 hours, than NWP.

On smaller urban scales, the REM quality is lower than on a continental scale since the smaller scales are less predictable (red stippled line). This entails that the NWP prediction will be more skilful at approx. 2-4 hours. The quality of the NWP model initiates lower than the REM prediction due to spin-up effects.

It is clear, from Figure 2, that there is a great potential in combining REM and NWP to increase the systems overall performance. The stippled green line conceptualises the outcome of combining a NWP model by assimilation of REM. The idea is that the higher quality of the REM prediction is beneficial for the NWP model when combined and not only in the assimilation period. This is the basis for the focus area of the Ph.D. on combining the two methods by assimilation.

An example of nowcasts generated by a Co-TREC REM and the Danish Meteorological Institutes (DMI) HIRLAM NWP model compared to the

corresponding observational radar precipitation field is seen in Figure 3. The example is from the previously described case that caused flooding in the Copenhagen area the 2nd July 2011.

REM nowcasted precipitation field
Prognosis issued 15:00 02-07-2011 UTC
+ 60 min lead-time

NWP nowcasted precipitation field
Prognosis issued 15:00 02-07-2011 UTC
+ 60 min lead-time

Observed radar precipitation field
16:00 02-07-2011 UTC
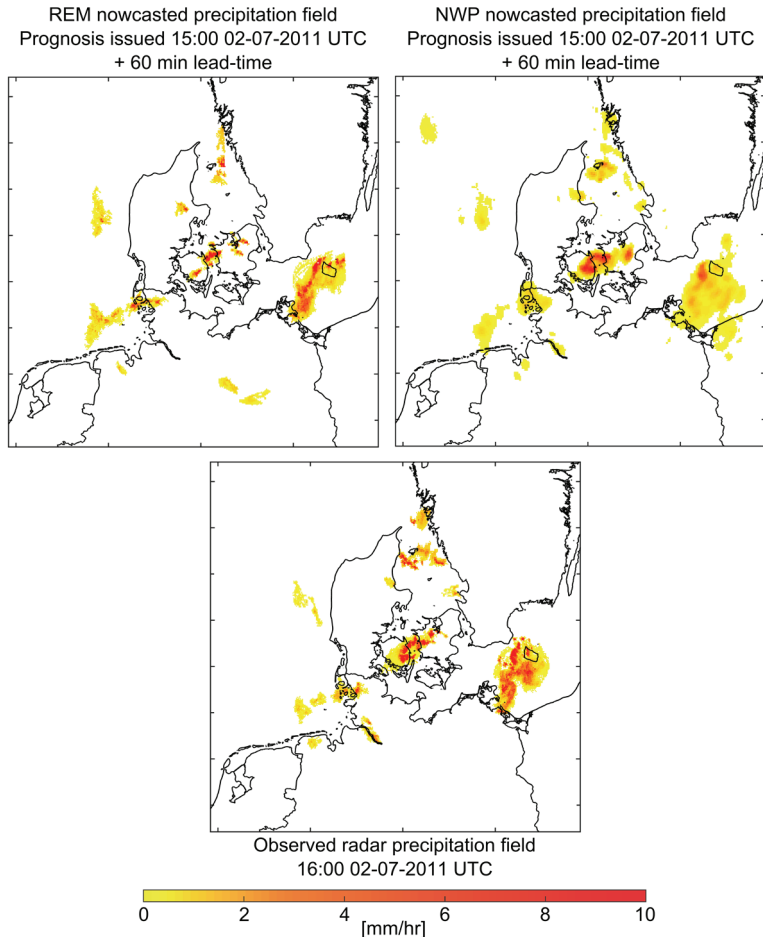
Figure 3: An example from nowcasts issued on the 2nd July 2011 15:00 UTC at lead-time 60 min from a REM and NWP model (DMI HIRLAM model) compared to the observational radar precipitation field. The plots depict the precipitation field from a minimum threshold of 0.5 mm/hr.

It is difficult to identify which one of the two nowcast methods has the highest quality. However, it seems that the REM prediction is more detailed on smaller scales than the NWP prediction. Common to both methods is that they are uncertain.

1.2. THE CHALLENGE OF NOWCAST UNCERTAINTY

The chaotic and transient nature of precipitation makes future predictions one of the most difficult earth system problems, and consequently among the most imprecise. Significant effort has gone into improving the performance of both REM and NWP methods but still predictions come with a significant amount of uncertainty.

Quantification of the nowcast uncertainty is very challenging and highly case dependent (Germann, Zawadzki et al. 2006) and also very much related to the nowcast methodology.

Extrapolating precipitation, as done by the REM method, is very simple, robust and fast. However, the quality of the prediction deteriorates rapidly as the method does not account for the temporal changes in precipitation (see Figure 2). As the quality deteriorates, the uncertainty increases. The uncertainty increases due to the non-stationarity assumption of the estimated motion field and foremost the evolution/decay of the precipitation (Germann, Zawadzki et al. 2006). This is also the reason why the quality for very short-lead times of REM is high and higher than the NWP models since the actual situation is the initial condition. The sources of uncertainty are further described in section 3.1.7.

NWP models simulate the atmospheric phenomena but there are model errors which affect the quality of the prediction. The prediction is challenging for two reasons. The first being the description of some physical processes that are related with uncertainty and secondly the temporal and spatial discretisation of the numerical approximation. Both are related to the computational power since a nowcast, in order to be useful, needs to be produced within a reasonable amount of time. Another issue is the non-linearity and the many degrees of freedom of the NWP methodology. Obtaining exact initial conditions from observations is not possible as they will be affected by uncertainties. The problem is that even slight changes in the initial states will very rapidly depart from each other and produce very different predictions (Lorenz 1965). These are the challenges for describing the future atmospheric state using NWP models.

Due to the uncertainty associated with nowcasting precipitation, there is an inherent risk in RTC. The uncertainty of the prediction has to be compared against potential consequences of incorrect control. Incorrect decisions based on wrong predictions of the precipitation can, in worst case, lead to flooding of urban areas with severe economic implications as a consequence. Quantitative estimation of the nowcast uncertainty before executing a control strategy is therefore very important and are therefore a focus area of this Ph.D. study.

The need to improve nowcasting at urban scales based on the three focus areas, with the aim of making predictions more applicable in RTC of urban drainage systems, has led to the following problem formulation and research questions.

1.3. PROBLEM FORMULATION AND RESEARCH QUESTIONS

It is clear from the previous descriptions that reliable and precise nowcasts are needed before they can be implemented successfully in urban drainage. Furthermore, uncertainty estimation is paramount before important control decisions, based on nowcasts, can be executed. Lastly there is a large potential in utilising the strengths of the two methods to improve the combined predictability and extend the lead-time of the nowcasts.

The motivation for further development of REM nowcasting methods is the applicability within RTC of urban drainage systems. Three focus areas have been identified; improve precision of REM prediction, utilise the strengths of the REM and NWP predictions by assimilation and quantify the nowcast uncertainty.

The above mentioned led to the main purpose of this Ph.D. study: *Improve nowcasting of 0-6 hour's lead-time for applicability in RTC of urban drainage systems*. This is done through working with the following research questions:

- How is it possible to improve the precision of deterministic REM nowcasting?
- The quality of a REM prediction, at urban scales, deteriorates rapidly so how is it possible to extend the lead-time?
- How can the nowcast uncertainty be quantified in a way that is applicable to RTC of urban drainage systems?

1.4. THESIS ORGANISATION

As a direct result of the research of the PhD project, a series of scientific papers and a technical note have been produced. Each paper or technical note represents individual research; a short overview are presented in the following subsection. The intention of the thesis is not to repeat, in details, the research presented in the papers but to give a summary of the main findings and to provide a retrospective overview. The thesis is structured in the following way:

Chapter 2 describes the basic principles of measuring precipitation by weather radars and the uncertainties related to the quantitative precipitation estimation (QPE).

Chapter 3 elaborates on selected REM nowcasts methodologies and state-of-the-art methods within the field of REM nowcasting.

Chapter 4 presents the work of the Ph.D. study that focuses on deterministic nowcasting. It elaborates on how Kalman filtering is implemented to temporally stabilise the advection field. The chapter also describes a developed methodology for vector retrieval by a variational technique and presents the results from assimilation of REM data into DMI HIRLAM NWP model.

Chapter 5 describes the work of the Ph.D. study to develop a REM ensemble prediction system called RESEMBLE and its performance when applied to the drainage system of the city Frejlev, Denmark. The chapter furthermore contains the results from initiating ensemble members in DMI HIRLAM NWP model by assimilation of RESEMBLE ensemble members.

Chapter 6 concludes the thesis and underlines the main findings of the research.

The scope of the work presented is nowcasting by REM. The thesis does not go into the further development of the NWP framework but instead works with the combination of the two methodologies of nowcasting by data assimilation. Data assimilation is a key stone in the overall project, by which the current PhD thesis is funded. The overall project is *HydroCast – Hydrological forecasting and Data assimilation*. The objective of the HydroCast project is to establish and test a general framework for hydrological forecasting and data assimilation that integrates different data sources with meteorological and hydrological modelling systems.

1.5. LIST OF SUPPORTING PAPERS AND TECHNICAL NOTES

Paper I: Jensen, D. G., Nielsen, J. E., and Rasmussen, M. R. (2015). *Does simple Kalman filtering improve the advection field of Co-TREC nowcasting?*

Paper II: Jensen, D. G., Petersen, C. and Rasmussen, M. R. (2015). *Assimilation of radar-based nowcast into a HIRLAM NWP model.*

Paper III: Jensen, D. G., Nielsen, J. E., Thorndahl, S. and Rasmussen, M. R. (2015). *Ensemble Prediction System based on Lagrangian extrapolation of radar derived precipitation (RESEMBLE).*

Paper IV: Jensen, D. G., Nielsen, J. E., Thorndahl, S. and Rasmussen, M. R. (2015). *Ensemble prediction of flow in urban drainage systems using RESEMBLE.*

Paper V: Jensen, D. G., Petersen, C. and Rasmussen, M. R. (2015). *Assimilation of ensemble radar based nowcast into HIRLAM NWP model for high intensity rainfall estimation.*

Tech. Note: Jensen, D. G. and Rasmussen, M. R. (2015). *Retrieval of advection fields using variational analysis techniques.*

All references, to the authors own work namely the above listed papers, is refereed in the following text as *Paper I* for Paper I etc. and *Technical Note*.

CHAPTER 2. RADAR BASED QUANTITATIVE PRECIPITATION ESTIMATE

The basis for all REM models is the radar QPE. In the following the basic working principles of measuring precipitation using weather radars are presented. Furthermore, possible error sources/uncertainties for radar QPE are described.

The radar is a remote sensing device that emits a signal and measures the backscatter from the signal as it hits a target. The name radar is an acronym for RAnge Detection And Ranging and was developed shortly before and during World War II to detect aircraft and ships for military purposes. It was noticed quickly that the radar also received additional interference, especially when it was raining. This lead to the further development of a more peaceful application of the radar namely to measure precipitation. The radar, since its invention, has undergone a significant evolutionary development to the state of the art radars of today (Rinehart 2010).

The radars of today is very complex in terms of hardware, signal generation and processing but the basic principle on how it works is easily understood. The radar, in essence, consists of three components. These are a transmitter, an antenna and a receiver. The transmitter sends out a high frequency electromagnetic wave emitted from the antenna, which travels at the speed of light. When the emitted energy hits an object, some of the energy is reflected. This reflected energy is then picked up by the antenna and processed in the receiver, which amplifies the signal to improve the signal-to-noise ratio.

The object position in space can be determined by knowing the exact position (azimuth and elevation) of the emitted signal, the speed of the electromagnetic wave and the time from transmission to receiving the signal. The main principle of the radar can be seen in Figure 4.
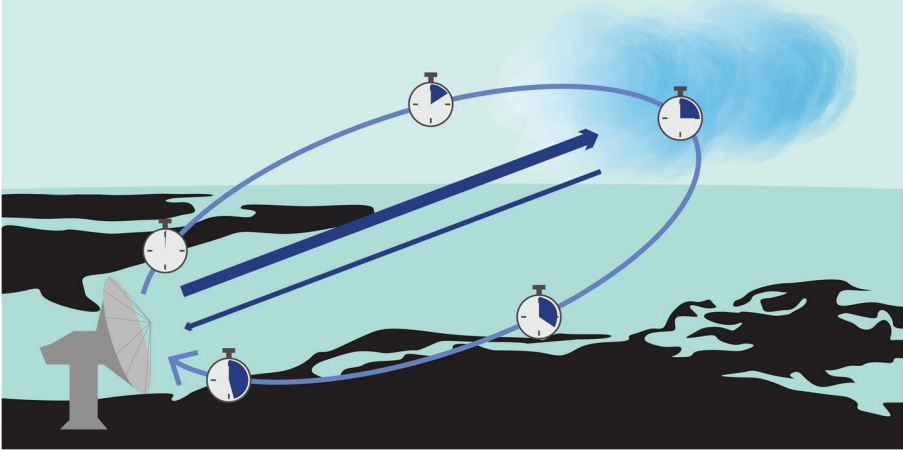
Figure 4: Basic principle of measuring precipitation by radar.

All measurement by weather radar is based on the radar equation that expresses the relationship between radar reflectivity of distributed meteorological targets and the received power (Battan 1959, Probert-Jones 1962, Battan 1973):

$$p_r = \frac{\pi^3 \, p_t \, g^2 \, \theta \, \phi \, h \, |K|^2 \, l \, z}{1024 \, \ln(2) \, \lambda^2 \, r^2} \tag{1}$$

Where p_r is the received power, p_t is the transmitted power, z is the reflectivity, g is the antenna gain, θ and ϕ are the horizontal and vertical beam width, h is the length of the pulse, λ is the wavelength and r is the radial distance to the radar. $|K|^2$ is the magnitude of the parameter related to refraction and l is the attenuation.

Most of the parameters of equation (1) are considered constant and are radar specific based on the setup and hardware. This applies to the transmitted power, pulse length and wavelength, antenna gain and the horizontal and vertical beam width. The parameter $|K|^2$ mainly depends on the target material but is also influenced by temperature and wavelength to a minor degree. Grouping these parameters together in a single parameter c by assuming that the only target is liquid precipitation will reduce equation (1) to the following expression:

$$p_r = \frac{c \, l \, z}{r^2} \tag{2}$$

The attenuation for C- and S-band radars is often neglected which simplifies the expression further. For this study, only data from C-band radars are used.

Equation (2) describes a relation between the returned power and the reflectivity, which is the basis for measuring precipitation. This is unfortunately not enough to

estimate the precipitation intensity. Here a relation between reflectivity and precipitation intensity is needed. The backscattering, and hereby also the reflectivity, is a function of the number and diameter of the precipitation droplets. The intensity of precipitation is also a function of the number and diameter of droplets, combined with their falling velocity. Since the falling velocity is a function of the drop size, this signifies that the precipitation intensity and the drop size distribution (DSD) are linked. This relation was utilised, by Marshall, Palmer (1948), to establish a relationship between the reflectivity (z) in logarithmic decibel domain (dBZ) and rainfall intensity (R), through an empirical power law as seen in equation (3).

$$z = \alpha R^{\beta}$$
(3)

This relationship has subsequently been verified by the work of Uijlenhoet, Pomeroy (2001). The value of the coefficients α and β, have been demonstrated to vary from event to event but also as a function of the specific event by comparing radar data with disdrometer readings (Lee, Zawadzki 2005). Furthermore, Lee, Zawadzki (2005) found that the instantaneous rain-rate estimation had a random error of 41%, which was decreased by daily accumulations to 28% using a fixed relation of $z = 210R^{1.47}$. The reason for this random error is that the relationship is in fact not constant.

Estimation of α and β, linked to the DSD, has been an important issue for over half a century (Marshall, Palmer 1948, Marshall, Hitschfeld et al. 1955, Joss, Waldvogel 1970, Richards, Crozier 1983, Smith, Joss 1997, Doelling, Joss et al. 1998, Uijlenhoet, Smith et al. 2003, Thompson, Rutledge et al. 2015). Despite the research, static parameters are often applied in operational use. The most often used set of parameters are

$$z = 200R^{1.6}$$
(4),

known as the standard Marshall Palmer coefficients (Marshall, Palmer 1948, Marshall, Hitschfeld et al. 1955). The uncertainty related to the non-static z-R relationship is normally handled by post processing the radar data by bias correcting the data to match ground observations. Several bias adjustment methods exist such as mean field bias adjustment at different timescales (Smith, Krajewski 1991) and conditional mean field bias adjustment as a function of precipitation intensity (Villarini, Krajewski 2010). Thorndahl, Nielsen et al. (2014) found over a 10 year period that hourly mean field bias adjustment showed the best performance.

The radar equation is derived assuming ideal conditions, which is not always the case. The uncertainties of radar QPE are not only related to the z-R relationship but also to a number of error sources illustrated in Figure 5.
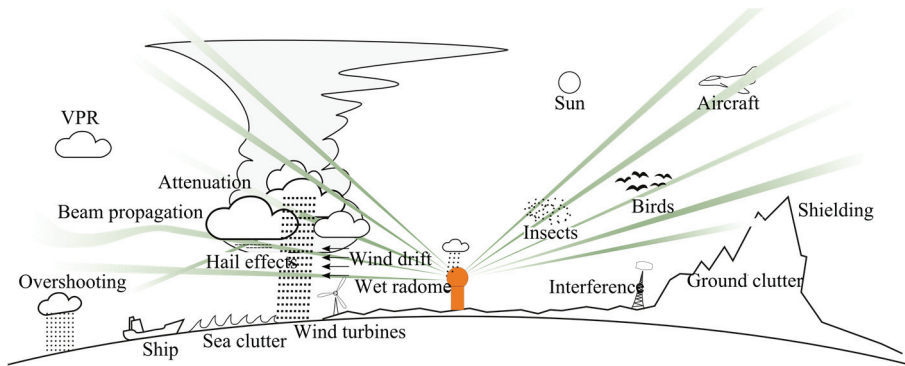
Figure 5: Error sources in measuring precipitation by radar, modified from Peura, Koistinen et al. (2006).

The error sources, if unfiltered, leads to presence of non-meteorological echoes in the radar precipitation field. This often causes severe overestimation of QPE. Some of the error sources are briefly described in the following.

Clutter, either ground or sea clutter, from mainly anomalous propagation of the signal is important to address. Different approaches have been developed, such as Harrison, Driscoll et al. (2000), Da Silveira, Holt (2001) and Sugier, du Chatelet et al. (2002), to detect and remove ground clutter with high success rates. Beam shielding or clutter in mountainous regions is especially problematic and several studies have given the problem attention by both deterministic and probabilistic approaches (Gabella, Notarpietro 2002, Germann, Galli et al. 2006, Germann, Berenguer et al. 2009).

The degree of beam attenuation depends on a number of factors; the wave-length of the radar (X-, C- and S-band), the intensity of the precipitation and the distance. For most C- and especially S-band radars, the attenuation is only a problem with very intensive precipitation. Attenuation is when the energy of the electromagnetic wave decreases as it travels through precipitation. The more intense the precipitation the more attenuation occurs. This causes an underestimation of precipitation intensity since the backscattered energy is reduced. Several correction schemes to take attenuation into account has been developed to give more reliable QPEs (Aydin, Zhao et al. 1989, Bringi, Keenan et al. 2001, Thorndahl, Rasmussen 2009).

Precipitation often forms high up in the atmosphere where the temperature normally is below the freezing point of water. The initial stage of the precipitation is in form of small ice crystals which then begin to fall towards the earth. As the precipitation falls through the atmosphere, the ice crystals go through different stages. The small ice crystals will continue to evolve into snowflakes and becoming increasingly larger until the temperature rises above the freezing point. At this point the exterior

of the snowflakes will start to melt and develop a water coating. Since water is approximately 10 times more reflective than ice, this will result in very high reflectivities due to the large size of the snowflake combined with the high reflectivity of water. This band of high reflectivities is called the bright band effect. As the melting continues does the snowflakes turn into water droplets and the reflectivity will be as "expected".

The vertical profile of reflectivity (VPR) is a function of the precipitation stages and identified as one of the dominant error sources by Joss, Waldvogel et al. (1990). This is a problem because the radar beam increases to measure higher and higher in the atmosphere as a function of the radial distance due to the refractive index and the curvature of the earth. For these reasons it is very important for correct QPE estimation to know; firstly the location of the bright band and secondly be able to classify which type of hydrometeor the beam is reflected from. If these two things can be detected, then it is possible to make corrections and estimate the QPE more precisely. Different approaches to take VPR into account have been developed that are conditioned on either seasonal factors (Koistinen 1991), precipitation type (Collier 1986), or on a typical shape of VPR (Gray, Uddstrom et al. 2002). Also more advanced methods based on statistical models which are range dependent (Krajewski, Vignal et al. 2011) or based on empirical knowledge (Cao, Hong et al. 2013) have been developed.

Lastly, external emitters that lead to interference in the received power, and other non-meteorological objects, can give incorrect measurements. Most of these unwanted reflectivities can be removed by various filters.

Nevertheless, despite the uncertainty, most radar data that has been proper adjusted, bias corrected and filtered from noise is highly useful and reliable data yielding high spatial and temporal resolution. This is also the reason for the increased popularity of weather radars being applied within hydrological modelling.

For this work it is assumed that standard Marshall Palmer without bias adjustment sufficiently describes the relationship between reflectivity and precipitation intensity. This is assumed since verification and validation is performed by comparing nowcast against radar observations. A bias adjustment of observations could lead to differences in adjustments between nowcasted data and observations making the validation invalid. However, for practical purposes, some sort of bias adjustment is necessary.

CHAPTER 3. NOWCASTING

In the following section, the basic principles of REM nowcasting are described in order to give an overview of the field. The basic principles are followed by a short review of selected nowcast systems that provide exemplary methodologies within the field.

3.1. REM PRINCIPLES

Different methodologies for REM nowcasting have been developed. Common to all methods are that they utilise one or more of the basic principles for prediction of future precipitation. In the following, the most central principles are described; Lagrangian persistence and optical flow, area tracking, cell tracking, spectral algorithms, ensemble prediction systems and REM uncertainty.

3.1.1. LAGRANGIAN PERSISTENCE AND OPTICAL FLOW

Before describing Lagrangian persistence it is necessary to explain the simplest form of predicting precipitation, which is Eulerian persistence. Eulerian persistence involves estimating the future state from the current state. This means that the advection field is set to zero and the source/sink term for the precipitation is likewise zero. This type of prediction is mostly used as a reference (Reyniers 2008).

Lagrangian persistence is when the advection field is not zero but the evolution of precipitation is zero (frozen precipitation field). In rigid coordinates can this be written as

$$u\frac{\partial P}{\partial x} + v\frac{\partial P}{\partial y} + \frac{\partial P}{\partial t} = 0 \tag{5},$$

where $P(x, y)$ is the precipitation intensity at (x, y) and u, v are the x- and y-component of the advection vectors, respectively. For Lagrangian persistence, $\frac{\partial P}{\partial t} = 0$ in Lagrangian coordinates (in the coordinates of the flowing system).

The precipitation field is known from the radar QPE but the advection field is unknown and has to be determined. Equation (5) is, within the context of computer science, called the optical flow (OF) equation. OF is defined as the apparent velocity of objects in an image.

Equation (5) contains two unknowns - u and v - and can therefore not stand alone in determining the advection field. Additional information is required in order to estimate u and v. The variational analysis technique introduces a cost function, as

in equation (6), which leads to an overdetermined set of respective equations within a neighbourhood (Ω) of each (x, y). Minimisation of the cost function estimates the advection field.

$$C = \sum_{\Omega} \omega \left(u \frac{\partial P}{\partial x} + v \frac{\partial P}{\partial y} + \frac{\partial P}{\partial t} \right)^2 \tag{6}$$

Here ω is a weighting factor utilising quality information that is an indication of the reliability for each (x, y) location (Peura, Hohti 2004). The weighting, defined either in pixel coordinates and/or neighbourhood coordinates, is important in order to avoid partially blocked rays or isolated cluttered pixels that can influence the vector retrieval.

Since the minimisation is not constrained, the estimation of the advection field is potentially unstable. Adding an additional equation is needed to provide sufficient information to ensure more reliable estimations of the advection field. The additional equation is called the optical flow constraint.

Different implementations of the OF method using a constraint for advection vector retrieval is used by Li, Schmid et al. (1995), Germann, Zawadzki (2002) and Bowler, Pierce et al. (2004) among others.

Even though the OF technique using a constraint for motion estimation is mathematically well-founded, the estimation of vectors is often noisy. This is typically because of precipitation evolution, which the OF technique is sensitive to. Other techniques for estimating the advection field, which are widely applied, are area tracking and cell tracking algorithms described in the following.

3.1.2. AREA TRACKING

One of the most implemented and extensively documented methodologies for advection vector retrieval is area tracking.

The basic concept of an area tracker is to divide a radar scan into equally sized grid boxes and determine the motion of each box from radar scan at time t to $t + 1$ within a maximum search area. The displacement of each box comprises the advection field.

Rinehart, Garvey (1978) developed a method called tracking radar echo by correlation (TREC) that uses the correlation coefficient to estimate the displacement of each box. The concept of TREC and most area tracking algorithms is illustrated in Figure 6.
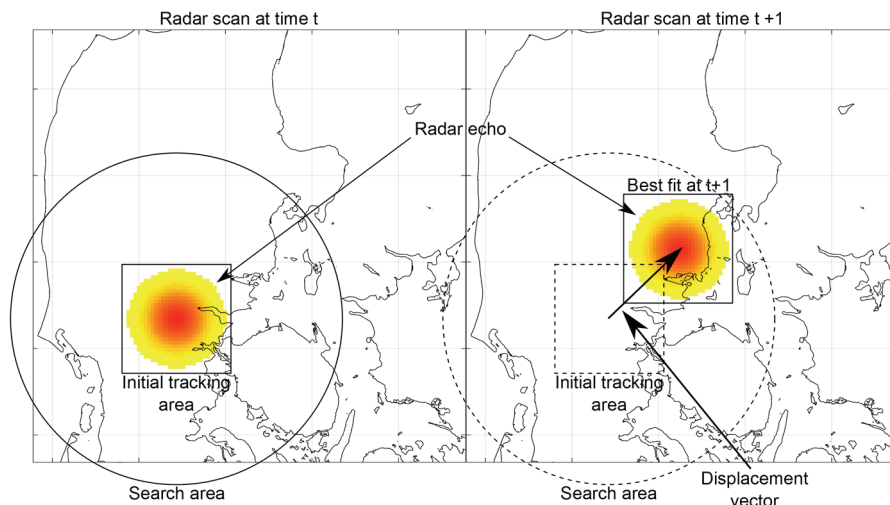
Figure 6: Conceptual illustration of the TREC methodology (In principle, most area tracking algorithms follow same procedure). The illustration is inspired by Mecklenburg, Joss et al. (2000).

Other area tracking algorithms are mostly variations of the TREC methodology. What differs from most area tracking algorithms is the way the optimum/minimum within the search area is computed. The TREC algorithm uses the 2D correlation coefficient, but other techniques such as mean square error (MSE), 2D standard deviation and 2D cross correlation can also be applied with similar results.

Unfortunately, because of evolution of the precipitation, the retrieved vectors are often noisy and even erroneous. Several methods for removal of erroneous vectors and spatial smoothing either by variational analysis, convolution using different filters or averaging of radar scans over time before motion estimation is applied to get more reliable estimates.

3.1.3. CELL TRACKING

Cell tracking algorithms are, by principle, different from area tracking and OF algorithms but often implemented in connection with one of the two. As the name implies, cell tracking (or centroid tracking) is a path estimation of precipitation cells (often convective cells).

For nowcasting, not only is tracking the cell path of interest but also the evolution as a function of time. This information is used to predict the future location and state of the cell. The advection of the cell can be done by simple linear extrapolation or more advanced methods as Kalman filtering (prediction). The

methodology is, because of the focus on cells, expected to perform well in convective situations compared to the area tracking approach (Reyniers 2008).

Every nowcast based on a cell tracking approach can be divided into two parts; a detection (segmentation) algorithm and a matching algorithm.

The detection algorithm segments the cell from the background. The segmentation methodology differs by using a single threshold or multiple thresholds to more advanced methods as nonparametric and unsupervised methods for automatic threshold generation either in 2D images or in 3D volume scans.

Cell characteristics are saved for each time step and used to match cells from subsequent time steps. The saved characteristics can be centroid coordinates, mean and max intensity, size, echo-top and vertical integrated liquid. Cell matching is usually performed within a search area defined by the previous cell advection velocity or by minimisation of a cost function weighting different characteristics of the cell (Dixon, Wiener 1993).

It is often observed that the cell dynamic behaviour is different from the larger enveloping area (Reyniers 2008) and that the cell moves in reference to the overall flow pattern (Li, Lai 2004). This is the reason why cell tracking and area tracking is often implemented jointly.

3.1.4. SPECTRAL ALGORITHMS

Several studies by Venugopal, Foufoula-Georgiou et al. (1999), Germann, Zawadzki (2002) and Surcel, Zawadzki et al. (2015) among others, demonstrate that the predictability of precipitation exhibits scale dependencies based on dynamic scaling processes. This means that smaller scales of the precipitation field usually have a shorter lifetime than larger scales and therefore makes them less predictable.

Spectral algorithms use this knowledge to decompose the precipitation field, by FFT or wavelet transformations, into a number of multiplicative cascades of different scales. The algorithm then extrapolates each scale according to their lifetime, often by weighting the specific cascade. As the scales are multiplicative in dBZ, demonstrated by Veneziano, Bras et al. (1996), it is possible to approximate precipitation fields by multiplying independent processes at different scales.

Decomposition of the precipitation field does not provide an estimate of the advection field, which is the reason why the methodology is coupled with other methods for vector retrieval and advection of the precipitation into the future. Spectral algorithms are used in nowcasting schemes such as STEPS (Bowler, Pierce et al. 2006), SBMcast (Berenguer, Sempere-Torres et al. 2011) and a newly

developed nowcasting algorithm by Atencia, Zawadzki (2014), which are described in more detail under section 3.2.

3.1.5. ADVECTION SCHEME

The advection scheme is an essential part of the nowcast methodology. The function of the advection scheme is to move the precipitation into the future according to the retrieved advection vectors.

Depending on how the advection is performed, the scheme has an influence on the preservation of small scale features and the spatial location of precipitation. Germann, Zawadzki (2002) made a comparison of four different schemes. The schemes were semi-Lagrangian forward, semi-Lagrangian backward, constant-vector backward and constant-vector forward. They concluded that the semi-Lagrangian backward interpolate once scheme had the smallest power loss of small scale features in the density distribution.

In a forward scheme, the parcel is advected downstream in space but forward in time whereas a backward scheme moves the parcel upstream in space but backward in time. There are pros and cons for each method: Forward schemes are mass conservative, meaning that the mean of the precipitation field is conserved in the nowcasted precipitation field. The problem with a forward scheme is how the parcel, advected into the future, is redistributed to the surrounding pixels since normally the future location does not coincide with a grid point. A backward scheme, on the other hand, is not strictly mass conservative (but close to) and since the scheme goes upstream in space, the parcel will always end in a grid point. The reason that a backward scheme is not mass conservative is because following the parcel backwards in time will normally not coincide in a grid point. The values are then found from interpolation of the surrounding values.

Semi-Lagrangian simply means that parcels "follows" the advection field. If the advection scheme is not semi-Lagrangian but constant, the same value is used for each parcel throughout the entire nowcast, whereas a semi-Lagrangian approach applies a new value for each time step according to the new location of the parcel.

Some of the problems with forward schemes can be minimised by performing the advection in a higher resolution than the original and applying a nearest neighbour interpolation once.

3.1.6. DETERMINISTIC AND PROBABILSTIC NOWCASTING

Deterministic nowcasts are, as the name implies, deterministic and therefore one "truth" is estimated. A quote of Albert Einstein says *"As far as the laws of mathematics refer to reality, they are not certain, and as far as they are certain,*

they do not refer to the reality" which, to some extent, applies to the deterministic nowcast since all predictions are uncertain.

The origin of nowcast uncertainty is described in more detail in the following section 3.1.7 and therefore only the two main principles of handling the nowcast uncertainty will be explained here.

The first method for addressing the uncertainty is by producing a future probability density function (PDF) of precipitation for each predicted pixel. Andersson, Ivarsson (1991), Schmid, Mecklenburg et al. (2000) and Germann, Zawadzki (2004) all developed such methods but the problem with this method is that they are not spatially or temporally correlated, which has been demonstrated by Zappa, Beven et al. (2010), to be crucial for hydrological modelling. This is the strength of ensemble predictions. Ensemble prediction gives a number of future possible predictions that are temporally and spatially correlated - in other words, a collection of deterministic nowcasts that forecast the forecast skill. The ensemble members are therefore directly applicable in hydrological modelling. Each ensemble member is weighted equally possible and therefore represents the uncertainty of the nowcast. This is also a weakness of the methodology since the probability of each ensemble member is unlikely to be equal in reality.

3.1.7. REM UNCERTAINTY

A more fundamental study of predictability and uncertainty by Germann, Zawadzki et al. (2006) identified three main sources of error for Lagrangian extrapolation nowcasts:

1. Growth and decay of precipitation not explained by the advection.
2. The nonstationarity of the motion field.
3. Model errors.

Germann, Zawadzki et al. (2006) additionally showed that the relative importance of uncertainty caused by (1) and (2) was case dependent.

The study was based on a definition of predictability by the concept of life time as derived by Germann, Zawadzki (2002). The lifetime (L) is defined as:

$$L = \int_0^\infty c(\tau) \tag{7}$$

With $c(\tau)$ expressed as:

$$c(\tau) = \frac{\iint_\Omega \hat{\psi}(t_0+\tau,x)\psi(t_0+\tau,x)}{\sqrt{\iint_\Omega \hat{\psi}(t_0+\tau,x)^2 \iint_\Omega \psi(t_0+\tau,x)^2}} \tag{8}$$

Where $\hat{\psi}$ is the nowcasted image, ψ is the observed radar image, t_0 is the start time, τ is the lead-time and $\boldsymbol{x}$ is the position. The computation of $c(\tau)$ is aggregated over the domain of the radar image (Ω). The life time is, in other words, based on the 2D correlation coefficient without subtraction of mean (Zawadzki 1973). If $c(\tau)$ follows an exponential law, then L will be the time of intersection between $c(\tau)$ and $1/e = 0.37$ (Germann, Zawadzki 2002).

The relative uncertainty related to applying a stationary motion field in Lagrangian persistence nowcasting was investigated by comparing the life time of (i) a stationary motion field and (ii) a nonstationary motion field. The nonstationary motion field was obtained as a series of motion fields updated for each observation along the lead-time of the nowcasts. This is obviously only possible in historical settings.

The results showed that L on average was improved by $1.1h$ using a nonstationary motion field compared to Lagrangian persistence. The life time for Eulerian persistence was found as $L = 2.9h$, Lagrangian persistence $L = 5.1h$ and using a nonstationary motion field resulted in $L = 6.2h$. The life time variations from event to event ranged from almost no improvement to approximately $2h$.

In the event that did not demonstrate any improvement using a nonstationary motion field, the uncertainty from the advection field was negligible compared to the growth and dissipation of the precipitation, and not because the motion field was stationary. This indicates that strong evolution of precipitation is the dominating factor but for events with less strong evolution, the nonstationarity assumption will become an increasing source of uncertainty.

The relative importance was also investigated by Bowler, Pierce et al. (2006) by comparing the mean square error (MSE) between a Lagrangian persistence nowcast and a nonstationary nowcast. They found that no significant differences in the MSE for lead-times up to 3 hours could be detected. When extending the lead-time to 360 min did the stationarity of the motion field only constitute 10% of the total nowcast error. This results align nicely with the findings of Germann, Zawadzki et al. (2006).

Both studies found a predominant role of uncertainty for the growth and evolution of the precipitation, which as mentioned, is case dependent.

The last sources of uncertainty are the model errors. The model errors are the sum of all inaccuracies in the estimation of the motion field, the discretisation in space, time and reflectivities and numerical errors originating from numerical diffusion of the advection scheme (Germann, Zawadzki et al. 2006).

The complete separation of errors originating from either growth and decay or nonstationarity of the motion field is highly complex for studies like the ones conducted by Germann, Zawadzki et al. (2006) and Bowler, Pierce et al. (2006). The reason for this is the model errors. One example is the estimation of the motion field, which also will suffer from the uncertainties related to growth and dissipation of the precipitation. In the estimation of the motion field, some vectors will be noisy and even erroneous due to false correlations caused by evolution and decay. This entails that the errors somehow are related or even correlated with each other.

The study of both Germann, Zawadzki et al. (2006) and Bowler, Pierce et al. (2006) was conducted on largescale mosaics with a fairly coarse spatial and temporal resolution. There is always a trade-off between spatial and temporal resolution in terms of the importance from the uncertainty of point (1) and point (2). Increasing the spatial resolution while maintaining the same temporal resolution will increase the uncertainty related to the assumption of the stationary motion field. How the interaction between spatial and temporal resolution affect the impact of uncertainty from (1) or (2) is an area where more research is needed. It was found by Nielsen, Thorndahl et al. (2014) that the temporal resolution is very important for the applicability and the accuracy compared to ground observations.

The point of developing nowcast systems is to address and minimise the uncertainty of growth and decay, the nonstationarity of the motion field and model errors. Many approaches have been developed both by improving the deterministic prediction but also by probabilistic approaches. To a certain degree, it is impossible to model all the processes going on in the atmosphere with REM based systems. It is therefore just as important to know and quantify the uncertainty.

3.2. DESCRIPTION OF SELECTED RADAR BASED NOWCAST SYSTEMS

Today, many nowcast systems exist that demonstrate great variety. These range from simple linear extrapolation models to systems that combine a number of different data sources and complex merging schemes. In the following, selected nowcast systems are described to give an overview of modern-day techniques within REM nowcasting.

TITAN
One of the most widely used models is TITAN (Dixon, Wiener 1993), which is based on a cell tracking approach (Reyniers 2008). The segmentation of cells from the background follows a fairly simple method. A fixed threshold of $T_Z = 35 \; dBZ$ and a volume of $T_V = 50 \; km^3$ is applied to the volumetric radar data in Cartesian coordinates to identify continuous regions classified as cells. The cell matching algorithm is based on minimisation of a cost function that weights two parameters,

d_p and d_V, which are the distances between cells and measure the difference in volume. The cost function is seen in equation (9) (Dixon, Wiener 1993).

$$C_{ij} = \omega_1 d_p + \omega_2 d_V \tag{9}$$

where,

$$d_p = \sqrt{\left(x_i - x_j\right)^2 + \left(y_i - y_j\right)^2} \tag{10}$$

and,

$$d_V = \left| V_i^{1/3} - V_j^{1/3} \right|. \tag{11}$$

Here (x, y) is the cell centroid coordinates and V is the cell volume for cell-indices (j, i). The matching of the cells are given by the minimisation of the cost function under constraint of the distance, which cannot exceed a maximum storm speed.

Merges and splits are also handled by the algorithm. When two cells merge into one, the new combined cell will have a weighted average of the merged cell weights. The position of merged cells are found from the predicted path of the now terminated cell(s) if the forecast position falls within the area of the merged cell. Splits are handled similarly: If more than one cell falls within the forecasted cell path area and has no history, then it is considered a split.

The extrapolation of cells are performed by a linear advection. Furthermore, the weighting property of the cell is also forecasted by an exponentially decreasing function back in time. This entails that the model is not mass conservative.

MAPLE
Another widely used nowcasting model is the McGill Algorithm for Precipitation Nowcasting by Lagrangian Extrapolation (MAPLE). The early development started in 1973 with a global vector approach (Austin, Bellon 1974). The method has been developed since and is today a much more advanced nowcaster. The methodology and implementation are described in a series of five papers (Germann, Zawadzki 2002, Germann, Zawadzki 2004, Turner, Zawadzki et al. 2004, Germann, Zawadzki et al. 2006, Radhakrishna, Zawadzki et al. 2012).
The retrieval of advection vectors follows a methodology based on a variational analysis technique which falls within the area tracking approach. This method is called Variation Echo Tracking (VET). The vector field is found by global minimisation of a cost function, J_{VET}, as defined in equation (12) (Germann, Zawadzki 2002):

$$J_{VET}(\boldsymbol{u}) = J_\psi + J_2 \qquad\qquad (12)$$

with

$$J_\psi = \int \int_\Omega \beta(\boldsymbol{x})[\psi(t_0, \boldsymbol{x}) - \psi(t_0 - \Delta t, \boldsymbol{x} - \boldsymbol{u}\Delta t)]^2 dx dy \qquad\qquad (13)$$

and

$$J_2 = \gamma \int \int_\Omega \left(\frac{\partial^2 u}{\partial x}\right)^2 + \left(\frac{\partial^2 u}{\partial y}\right)^2 + 2\left(\frac{\partial^2 u}{\partial x \partial y}\right)^2 + \left(\frac{\partial^2 v}{\partial x}\right)^2 + \left(\frac{\partial^2 v}{\partial y}\right)^2 + 2\left(\frac{\partial^2 v}{\partial x \partial y}\right)^2 dx dy$$
$$(14)$$

where u and v are the x- and y-component of the advection vector, respectively. $\beta(x)$ is a data quality weight for each pixel in the observed radar scan ψ at time t_0 and $t_0 - \Delta t$ for domain Ω. J_ψ is the square of the residual error of Lagrangian persistence as described by equation (1). J_2 is a smoothness penalty function (Wahba, Wendelberger 1980) that influences the minimisation of the nonlinear cost function by the degree of divergence/convergence that is accepted. The influence of J_2 is weighted by γ.

An initial guess is needed to ensure convergence towards a global minimum. In a start-up situation, this done iteratively by gradually increasing the number of vectors to estimate. The first guess using global vector results from the minimisation is in advection vectors with a higher temporal resolution of, for example, 5x5 vectors. The 5x5 vectors are again used as initial guess for the next iteration, which yields an even higher resolution of advection vectors. This procedure is continued until the desired resolution is obtained. In a real-time situation, the last estimated vector field is used as an initial guess.

The advection of precipitation is performed by a semi-Lagrangian backward interpolate once scheme as described in 3.1.5.

MAPLE also implements a method to obtain the probability of a forecasted value to exceed a given threshold called "Local Lagrangian" probability forecast (Germann, Zawadzki 2004). The method determines the density distribution from parcels around the pixel to construct a probability. The advantage of such a system is that the probability of exceeding a threshold for a given lead-time can be used to issue a warning of flooding, landslides and other costly and unfortunate events. The drawback is that no spatiotemporal correlation exists and the nowcast cannot directly be applied in hydrological models.

Lastly, a wavelet transform is implemented to separate the small-scale precipitation and ensure it is not nowcasted beyond its life time (Turner, Zawadzki et al. 2004).

The different spatial-scales are weighted as a function of lead-time. The weighting function is determined by the life time estimated by a posteriori analysis where the life time is estimated at different cut-off wavelengths by correlation of Lagrangian persistence nowcasts against observations. The lifetime is estimated when the 2D correlation coefficient drops below $r = \frac{1}{e} = 0.37$. A linear relationship is found and this information is used to extrapolate precipitation to, but not beyond, its life time.

STEPS
The idea of not predicting spatial scales beyond its life time is also one of the core concepts for the model Short-Term Ensemble Prediction System (STEPS) (Bowler, Pierce et al. 2006). STEPS is one of the more advanced nowcasting models that combines an REM and NWP model. The model is based on combining "cascades" from three sources: a noise cascade, REM cascade and NWP cascade. A cascade is the decomposition of the radar scan or the NWP predicted precipitation field into structures of different scales. The REM of STEPS is a modified version of the model developed by Seed (2003) called Spectral Prognosis (S-PROG).

S-PROG develops cascades from a decomposition of the radar scan in dBZ by FFT. The life time of each level in the cascade is found as a least square fit to a power-law relationship as a function of scale. The life time of each scale is estimated by comparing a Lagrangian persistence nowcasted scale with the same corresponding observed scale. This relationship is used to inject spatially and temporally correlated noise into a specific scale when that scale loses skill.

The last cascade originates from the nowcasted NWP model. This ensures that the precipitation nowcast evolves towards the large dynamical evolution of the atmosphere (Reyniers 2008). The final nowcasted precipitation field for a given lead-time is constructed by the three cascades. The procedure is that each scale is combined from the three cascades by weighting each component. More weight is given to the REM model for very short lead-times and the NWP prediction is gradually weighted more. The noise follows the fitted power-law function such that noise is firstly injected into the small scale features and at longer lead-times it is also injected into the larger scales. Lastly, it is renormalised to correct the power loss of small scale features since these will become increasingly more uniform over time (Bowler, Pierce et al. 2006).

The advection field in STEPS is estimated using a OF approach (Bowler, Pierce et al. 2004) based on the Horn, Schunck (1981) method. The method can be sensitive to large displacements, which have been avoided by translating the image according to a single displacement vector prior to the motion estimation by OF. Because of considerable noise in the estimation of the advection vectors, they are subjected to an exponential smoothing in time following the form:

$$\boldsymbol{v}_{smooth}(t) = \alpha \boldsymbol{v}_{smooth}(t - \Delta t) + (1 - \alpha) v_{estimate}(t) \qquad (15),$$

where $\boldsymbol{v}_{smooth}$ are the smooth advection vectors, $\boldsymbol{v}_{estimate}$ are unsmoothed advection vectors and α is an exponential parameter given the time scale of the smoothing (Bowler, Pierce et al. 2006). A value of $\alpha = 0.85$ is chosen, which gives a smoothing time scale of approximately 90 min. The advection scheme is backwards in time.

The ensemble generation of STEPS is based on introducing randomly generated noise fields for the small scale features in the S-PROG forecast cascade and introducing a random component to the advection field. This is done for each different ensemble member.

Lately, STEPS has been extended to also include radar observation errors, the choice between two noise generators - a parametric and a non-parametric - and the possibility to combine a number of forecasts from different sources (Seed, Pierce et al. 2013).

SWIRLS
The Short-range Warnings of Intense Rainstorms in Localized Systems (SWIRLS) is, as the name implies, optimised for heavy precipitation events (Li, Lai 2004). The method combines both an area tracking and cell tracking algorithm. This is done since it is often observed that convective cells move in reference to the overall flow pattern. The area tracking approach is based on the TREC methodology described in section 3.1.2. The further processing of the TREC vectors has much similarity with the Co-TREC methodology (Li, Schmid et al. 1995) but with some discrepancies. SWIRLS identifies erroneous vectors as vectors that deviate more than 25 degrees from the surrounding 25 vectors whereas Co-TREC makes a similar comparison with 9 vectors. Both methods incorporate a spatial smoothing of the vector field to avoid divergent flow fields. SWIRLS uses a Cressman objective analysis method (Cressman 1959) that is somewhat similar to the variational analysis approach opted for in Co-TREC.

The cell tracking approach is similar to the segmentation methodology of TITAN where a single threshold is applied and the cell is being represented by an ellipse. The cell path is computed by identifying similar sized cells within a search radius, found from the predicted future cell location, that do not have a directional change exceeding 90 degrees.

The SWIRLS model was developed in Hong Kong, which experiences very heavy showers during the monsoon time. It is well known that the Z-R relationship is not static and using standard Marshall Palmer (Marshall, Palmer 1948) coefficients of $a = 1.6$ and $b = 200$ can lead to significant bias depending on the drop size distribution (Lee, Zawadzki 2005). This is especially true in heavy precipitation. For these reasons, SWIRLS implements a real-time Z-R correction for QPE based on rain gauges in the greater area of Hong Kong. The Z-R correction is done with a

temporal resolution of five minutes and for each rain gauge corresponding to an area of the radar scan. This is a unique feature of the SWIRLS system.

SBMcast
The SBMcast (Berenguer, Sempere-Torres et al. 2011) is an ensemble based nowcast model. The advection vectors are retrieved by the Co-TREC methodology (Li, Schmid et al. 1995), which is an area tracking approach. Only the evolution uncertainty is described in this model and is based on the "String of Beads Model" (SBM) by Pegram, Clothier (2001b) and further developed for time series mode in (Pegram, Clothier 2001a). SBMcast produces ensemble nowcasts to describe the evolution uncertainty that has similarities with the methodology of STEPS.

The original SBM can be used to generate a number of realistic stochastic precipitation fields that have the same properties as the corresponding observed precipitation fields in terms of Wet Area Ratio (WAR), Image Mean Flux (IMF) and spatial correlation β_{space}. WAR is the proportion of precipitation field above a certain intensity threshold (in SBMcast $1\frac{mm}{h}$) and IMF is the average precipitation rate. The spatial correlation is modelled by the parameter β_{space}, which is estimated as the power exponent in a linear fit, in log space, to the radially averaged spatial power spectrum obtained from the observational precipitation field.

Pegram, Clothier (2001a) showed that WAR and IMF are closely related to the mean μ and spread σ of a fitted lognormal distribution to the observed precipitation rates, which makes it possible to stochastically generate a precipitation field with a correct lognormal distribution from only the three parameters (WAR, IMF and β_{space}).

The parameters WAR and IMF are extrapolated (1D) into the future by an AR(5) model by adding a stochastic component computed from the covariance of WAR and IMF to ensure second-order stationarity. This does, to some extent, model the evolution of the precipitation field for the individual ensemble members. The number of WAR and IMF is equal to the number of ensemble members and one value per lead-time is obtained. β_{space} is held constant since it was demonstrated that the parameter is close to having temporal persistence.

A stochastic precipitation field is generated by the following sequence (Berenguer, Sempere-Torres et al. 2011):

1. Convolute a white noise field Y with the same size as the precipitation field by a power-law filter based on β_{space}. (FFT Y, perform the filtering, and inverse FFT Y which is now spatially correlated).

2. Ensure that the precipitation field has the correct WAR as predicted (nowcasted) by estimating a in $\widehat{\boldsymbol{R}} = R_{th} e^{(Y+a)}$, where R_{th} is the precipitation threshold and $\widehat{\boldsymbol{R}}$ is the stochastic generated precipitation field (non-"bias" corrected).

3. Force the IMF of the stochastically generated precipitation field to have the same IMF as predicted for the given lead-time by estimating $\Lambda(t)$ of $\boldsymbol{R} = R_{th} \left(\frac{1}{R_{th}} \widehat{\boldsymbol{R}} \right)^{\Lambda(t)}$, where $\boldsymbol{R}$ is one precipitation field in the ensemble generation.

The SBMcast uses this stochastic approach to generate ensemble members. The temporal correlation is ensured by an AR(2) model including the observations to insure a realistic transition from observation to nowcast. The parameters of the AR(2) model are estimated by the Yule-Walker equations and are similar to the one used by Germann, Berenguer et al. (2009). The temporal correlation is added before the extrapolation and therefore mimics the temporal persistence in a Lagrangian coordinate system.

The final step is to advect the generated ensemble precipitation fields according to the backward semi-Lagrangian interpolate once scheme where the advection field is assumed stationary throughout the nowcast.

Lagrangian Ensemble Technique
Atencia, Zawadzki (2014) have developed a nowcast model that is based on a spectral algorithm with some similarities of both STEPS and SBMcast. The method is described in Atencia, Zawadzki (2014), which is the first in a series of articles comparing different nowcasting techniques.

The advection field is obtained using the Co-TREC methodology (Li, Schmid et al. 1995) and advected by a semi-Lagrangian backward scheme (Staniforth, Côté 1991). The ensemble generation, based on FFT, is divided into two steps to ensure that the phase and amplitude of the ensembles match that of the observation. In this context, the phase and amplitude can be perceived as a temporal and spatial component of the realisation, respectively.

The phase of the ensemble is simulated by finding a proper wavelength cut-off from low-pass filtering of the latest observation. The contours of the low-pass filtered reflectivity are used to generate a no-rain probability map. A noise field that is spatiotemporally correlated is generated. This noise field is only temporally used to obtain a future precipitation mask by multiplying the no-rain probability, after thresholding and normalisation, with the noise field. The mask is nowcasted into the future according to the advection field. The shape of the mask, based on the large scale features of the observations, introduces anisotropy into the predicted fields and also predicts which pixels should be temporal correlated in Lagrangian

coordinates as a function of lead-time. The temporal correlation is obtained using a conditioned second order auto-regressive model.

The procedure of creating the precipitation field, inside the nowcasted mask as a function of lead-time, is done by reproducing the power spectrum of the last observed reflectivity field through an iterative process. Firstly, a generator is created to reproduce the correlation of the last observed reflectivity field and secondly, a white noise field is convolved using the generator which ensures spatially correlated noise. Lastly the new correlated noise field is masked with the estimated mask, which introduces the phase information. These three steps are then repeated. A new generator needs to be created for every iteration since the new masked correlated field does not have the same correlation as the previous (but similar phase). The iterative procedure is repeated until both the slope of the power spectrum and the mean of the masked correlated field vary by less than 0.1% between each iteration.

This procedure ensures ensemble members that have both the same power-spectrum slope and similar anisotropy as the Lagrangian nowcast. The difference from this methodology to the one of STEPS and SBMcast is that the focus is also on the phase and not only on the amplitude (power-spectrum).

3.3. COMPARISON OF NOWCAST PERFORMANCE

As demonstrated above, many different nowcast systems have been developed and several more exist other than those described. Each system is developed for a specific radar configuration and location, which makes it difficult to compare the performance of different systems directly. Regardless, two efforts have been carried out in order to compare the systems; one in Sydney 2000 and another in Beijing 2008 in the context of the Olympic Games.

The comparison in 2000 called the Sydney 2000 Forecast Demonstration Project (FDP) (Wilson, Ebert et al. 2004, Pierce, Ebert et al. 2004) was run for three months at Australian Bureau of Meteorology (BoM). The tested systems were TITAN, NIMROD (Golding 1998), GANDOLF (Pierce, Hardaker et al. 2000), ANC (Mueller, Saxen et al. 2003) and S-PROG of which TITAN and S-PROG is described previously. GANDOLF and NIMROD were developed at the U.K. Met Office and are jointly operated. NIMROD is the default system in stratiform precipitation situations but when mass air convection is present, GANDOLF is activated. NIMROD is a combination of REM and NWP whereas GANDOLF is an object-oriented expert system that also uses NWP data for retrieval of advection vectors. ANC, developed at the National Center for Atmospheric Research (NCAR), is likewise an expert system that combines numerous data sources such as radar reflectivity, Doppler scans, satellite images, mesonet weather station data,

soundings, and so on. Also, the methodology of TITAN and TREC is incorporated into the ANC system.

The 2008 Beijing FDP (Wang, Keenan et al. 2009) was trialled over a time period from mid-July to mid-October 2008. The demonstration models were BJANC (Mueller, Saxen et al. 2003), CARDS (Joe, Falla et al. 2002), GRAPES-SWIFT (Xue, Droegemeier et al. 2007), MAPLE, NIWOT, STEPS, SWIRLS and TIFS (Bally 2004) of which MAPLE, STEPS and SWIRLS are describe previously. BJANC is the same ANC model used in the Sydney 2000 FDP but adapted to the Beijing area. CARDS is the operational radar processing system from Canada. The system contains, among other things, a Lagrangian extrapolation model based on area tracking. GRAPES-SWIFT is likewise a Lagrangian extrapolation model (Co-TREC), but which is blended with a NWP model for longer lead-times. NIWOT, without an official reference, is also a Lagrangian extrapolation model combined with an NWP model, which additionally has the possibility for human interference on the prediction. Lastly TIFS is a "poor man's" ensemble of the contributing systems (BJANC, CARDS, GRAPES-SWIFT, MAPLE, STEPS, and SWIRLS) (Wang, Keenan et al. 2009).

The conclusion from the Sydney 2000 FDP, according to Pierce, Ebert et al. (2004), was that Lagrangian persistence methodologies are generally superior to more sophisticated, nonlinear nowcasting methods. In convective scenarios, cell tracking systems perform the best but area tracking methodologies are better in stratiform situations.

In the Beijing 2008 FDP, a verification tool "The Real Time Forecast Verification" (RTFV) developed at the Australian BoM was implemented. RTFV computes a number of standard skill scores such as root mean square error and contingency table based scores. Also diagnostic verification methods are supported, such as feature-based verification, fuzzy logical verification methods and intensity scale verification.

Eight years have separated the two FDPs and several new systems have been developed while other systems have been upgraded. For these reasons, it is interesting when comparing the results from Beijing 2008 FDP with the Sydney 2000 FDP because it shows the track errors of convective cells have not improved. The track errors are the distance between nowcasted and observed cells. The results show that none of the present systems are better to predict the location of the convective cells than those available in 2000. Major improvements are, on the contrary, demonstrated when looking at the Critical Successive Index (CSI) for deterministic quantitative precipitation forecasts (QPF). The most likely explanation for the CSI improvement is that the nowcast schemes are better than they were in 2000 for non-convective situations and not that the weather in Beijing is easier to predict since the cell distance error was not improved. Overall, it seems

that STEPS stands out as being the most precise nowcast system even though a bias is present between the observed and nowcasted intensity distributions.

Another conclusion from the Beijing 2008 FDP is that probabilistic nowcast systems bring more knowledge compared to deterministic nowcasts. The strong performance of nowcasted precipitation amount and thunderstorm strike probability suggests that the probabilistic approach is more applicable. The probability value also provides better information for decision making. (Wang, Keenan et al. 2009).

CHAPTER 4. IMPROVING DETERMINISTIC NOWCASTING BY KALMAN FILTERING AND ASSIMILATION

Most probabilistic nowcast systems as those described in section 3.2 build upon a deterministic component. It is therefore of great importance to develop the deterministic part of the nowcast system in order to minimise the uncertainties as much as possible to give the best foundation for probabilistic predictions.

The first part of the Ph.D. study focuses on improving the stability and quality of the deterministic part of REM nowcast systems and combining REM and NWP predictions.

With regard to REM nowcast systems that follow the Lagrangian persistence approach, it is natural to focus on the estimation of the motion field. The reason for this is that it was concluded from the two demonstrations projects, described in Section 3.3, that the spatial estimation of cells was not improved from year 2000 to 2008. Furthermore, the evolution is not part of the Lagrangian persistence methodology where the latest radar precipitation field is extrapolated into the future but remains persistent. However, some morphological changes will occur due to the extrapolation following the advection vectors either from acceleration/de-acceleration and convergence/divergence in the flow pattern. This entails that the original image will be distorted to a slight degree.

As part of the Ph.D. study, a Lagrangian persistence model based on the Co-TREC methodology (Li, Schmid et al. 1995) has been developed called RES (Radar Extrapolation System). This model is used as a research platform for the work described in *Paper I - V* either for further development or as a basis for probabilistic predictions.

The Co-TREC methodology estimates the advection vectors as presented in Figure 6. The displacement vectors, based on the 2D correlation coefficient, are found from one box in image 1 at time $t-1$ to image 2 at time t. The result is the raw TREC vectors (Rhinehart 1981) which, due to growth and dissipation uncertainty from image 1 to image 2, can be noisy and even erroneous. The Co-TREC methodology is two-pronged; firstly is erroneous vectors identified and deleted and secondly a variational technique is implemented to spatially smooth the vector

field and ensure continuity and zero divergence over the measured domain (boundaries).

The erroneous TREC vectors are identified as deviating more than 25 degrees from the mean direction of the surrounding vectors. In practice, vectors that deviate too much are flagged and all vectors are checked for this condition before any vectors are deleted. This ensures that the identification sequence does not influence the identification.

The variational technique applied is described by (Sherman 1978) where a minimisation of a cost function returns Co-TREC vectors that are as close to the original TREC vectors as possible but still fulfil the imposed dynamical and statistical constraint. This technique has several similarities with approaches applied within optical flow techniques and the MAPLE VET methodology.

The solution of the variational analysis is the minimisation of a cost function, equation (16), under the constraint of continuity equation (17) (two-dimensional Boussineq mass continuity equation).

$$J(u,v) = \int_{\Sigma} \ [(u - u_0)^2 + (v - v_0)^2]dxdy \qquad (16)$$

$$\frac{\partial u}{\partial x} + \frac{\delta v}{\delta y} = 0 \qquad (17)$$

The advection scheme is a semi-Lagrange interpolate once forward scheme. Referring to subsection 3.1.5, a backward scheme would have been better in terms of always ending a parcel within a grid point. For computational reasons, the forward scheme, following some matrix operations, can be computed very efficiently. The advection is performed in a sub-resolution of 200 m compared to the original resolution of 2000 m, ensuring that the disadvantages in a forward scheme are minimised and negligible. Using a sub-resolution also ensures that the numerical dispersion is low. The precision of the advection vectors, when interpolated into the resolution of the radar, are finer than the original resolution of the radar. Performing the advection in a more fine resolution can utilise this higher precision better and hereby produce smoother advection.

4.1. PAPER I: DOES SIMPLE KALMAN FILTERING IMPROVE THE ADVECTION FIELD OF CO-TREC NOWCASTING?

From the review of the nowcast systems, section 3.2, the only model that applies temporal smoothing of the advection field is STEPS. Almost all nowcast systems uses some kind of spatial smoothing and filtering but not temporally. In the STEPS methodology, temporal smoothing was found necessary even with large spatial

smoothing applied to the precipitation fields prior to motion estimation. An exponential temporal smoothing is implemented in STEPS with a time-scale of 90 min. Studying advection fields over time produced by the developed Co-TREC based nowcaster, described previous, reveals some of the same challenges with noisy vectors as observed by Bowler, Pierce et al. (2006). An example of this is illustrated in Figure 7.
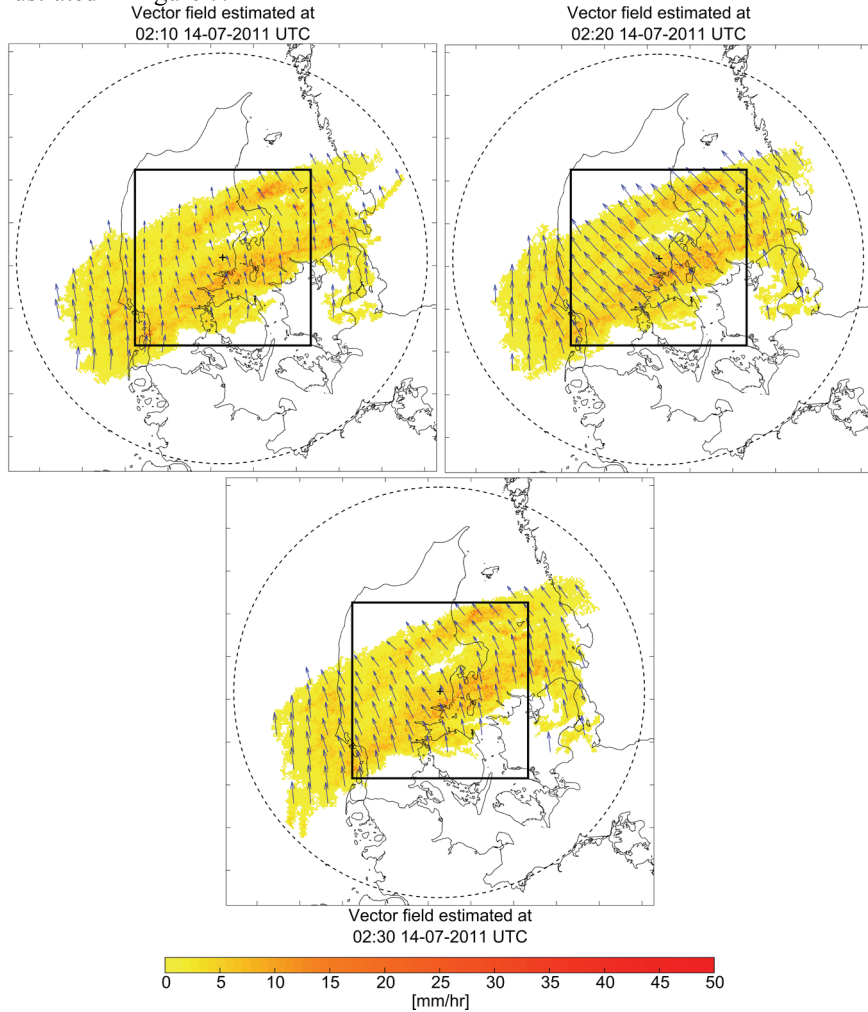
Figure 7: Example of temporal changes in direction of advection vectors from three time steps overlaid the radar precipitation field from Virring radar, Denmark. Within the rectangular box has vectors changed almost 45 degrees from one time step to the next including a dramatic change in speed. Top left image is from the 14th July 2011 at 02:10 UTC, the top right is next time step at 02:20 UTC and the bottom image is the last time step at 02:30 UTC. The plots depict the precipitation field from a minimum threshold of 0.5 mm/hr.

These changes over time are not physically based but more an expression of the uncertainty in estimating the advection field. The topic of *Paper I* in the Ph.D. study is how to handle these changes over time, in direction and speed, of the advection vectors.

The basic idea of *Paper I* is to temporal filter the advection field constrained by physical changes. For these reasons was it chosen to use a Kalman filter with a constant acceleration model using the standard Kalman update equation (Hwang, Brown 1997) and calibrate it against the physical changes in radial velocity measured by Doppler radar.

More specifically, the advection field from 16 events were converted into radial velocities. The changes in radial Co-TREC velocity from time step t to $t + 1$ were then compared with the changes in Doppler velocities. Hereafter, the Kalman filter was calibrated so that the level of Co-TREC radial velocity change matched the observed change.

Furthermore, it was investigated how two methods for identification of erroneous vectors influenced the results. The first method, being the more restrictive, identified vectors that deviate more than 25 degrees from the surrounding vectors as erroneous (REV>25), which is the original Co-TREC method, whereas the second method was 100 degrees (REV>100).

The Kalman filtering worked as expected by filtering out the noisy fluctuations in direction and speed of the advection vectors as demonstrated in Figure 8.
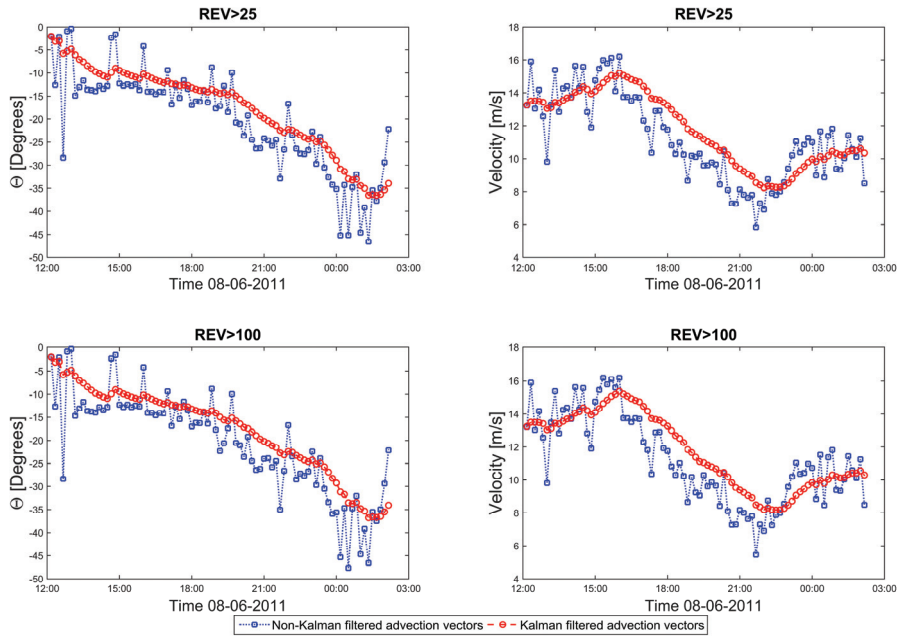
Figure 8: Changes over time of centre advection vector in direction and speed from an event on 08-06-2011. Both Kalman filtered (red) and non-Kalman filtered (blue) for each of the two erroneous vector identification methods are illustrated.

Besides the temporal filtering of the Kalman filter, it is noticeable how little effect the restricted and less restrictive identification and removal of advection vectors has for this specific example, REV>25 and REV>100 respectively. This is good since it indicates that the advection vectors are noisy but only with minor fluctuations at least less than 100 degrees from the surrounding vectors most of the time. However, it should be noted that for some of the other evaluated events there was larger fluctuations which created more pronounced differences between the two methods.

Comparing pooled skill scores as a function of lead-time for non-Kalman filtered nowcasts and Kalman filtered nowcasts did not reveal any significant differences in performance. The positive contribution from applying temporal Kalman filtering is stability improvements, which is also important for RTC of drainage systems. The relative standard deviation showed that the Kalman filtered nowcasts were more stable which, in practice, means that prognoses that are performance outliers can be avoided. This naturally goes both ways, since outliers in both ends of the spectrum is avoided. Stability is important for the applicability of the nowcasts in real-time.

To demonstrate the effect of the Kalman filter, the same situation as seen in Figure 7 is illustrated in Figure 9 with the difference that the temporal Kalman filtering is applied.
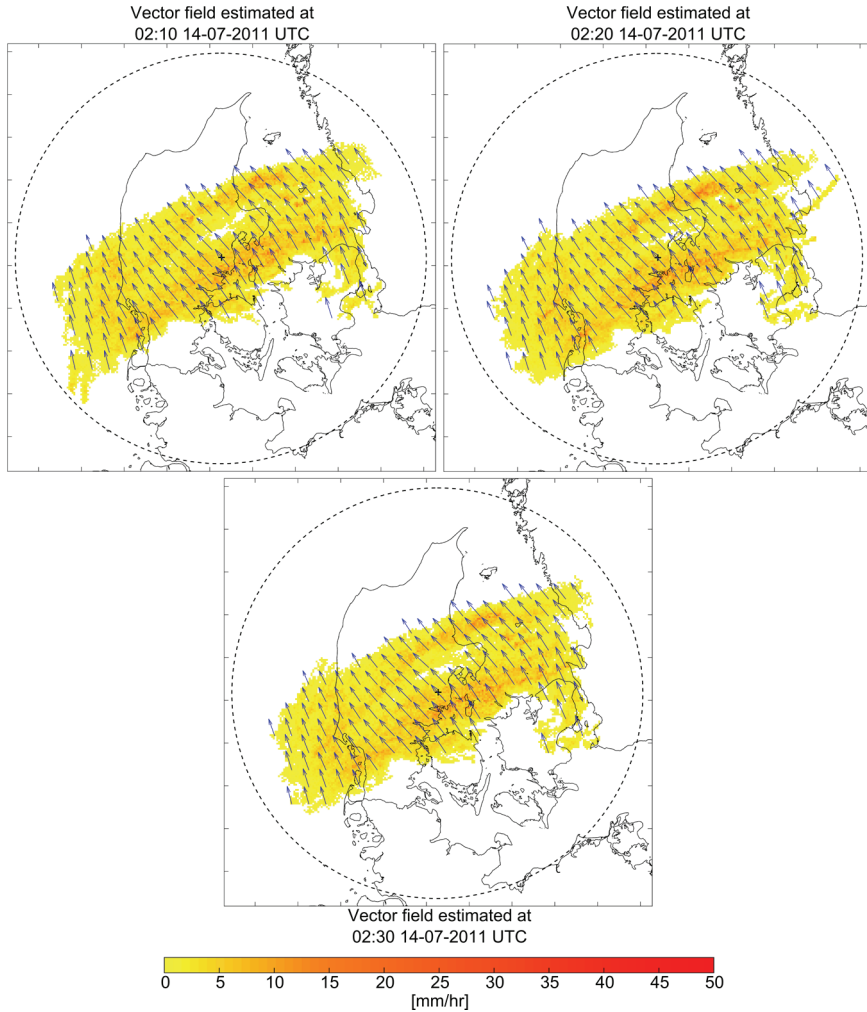
Figure 9: Same as in Figure 7 but with a Kalman filter applied. The plots depict the precipitation field from a minimum threshold of 0.5 mm/hr.

Figure 9 clearly shows the effect of the temporal filtering. The changes over time are not as dramatic as the one presented in Figure 7.

Inherent in the Kalman filter is also the possibility for predicting the future state of the advection system and not only temporal filtering. This was one of the main

reasons for choosing this kind of filter. By predicting the development in the advection field, the uncertainty originating from the nonstationary assumption of the advection field would be addressed. Due to the fairly slowly changes in direction and speed of the advection, this would probably be possible to predict successfully. Future work will try to apply the same calibration of the Kalman filter based on Doppler velocities to predict the development in the advection field as a function of lead-time.

4.2. TECHNICAL NOTE: RETRIEVAL OF ADVECTION FIELDS USING VARIATIONAL ANALYSIS TECHNIQUES

Another approach for advection field estimation, as presented in *Technical Note I*, was also developed to investigate other possibilities for handling the uncertainties when estimating the advection field. The new methodology, for vector retrieval is based on a variational technique, and differs from the method of Co-TREC but is still considered an area tracking approach. The method has similarities with Variation Echo Tracking (VET) as described in section 3.2 by applying the same smoothness penalty function as introduced by (Wahba, Wendelberger 1980).

The advantages of this method, compared to the Co-TREC method, is that the convergence/divergence can be controlled directly in the estimation of the advection field. In the Co-TREC method the final result is obviously highly influenced by the estimation of the TREC vectors and hereby also the ability to identify erroneous vectors, which for some situations can be complex. This is not a problem if single vectors slip through the identification (the method is developed to overcome this) but if small clusters of vectors are not identified as being erroneous, then this will have a large impact on the final estimated advection field. Another important aspect of the vector retrieval method is that it will estimate the overall flow pattern. Depending on the needed spatial scale this can both be positive and negative.

The disadvantage of the new method is that the solution to the minimisation can be caught in a local minima and not the global minima resulting in false advection fields. This is also the reason why an iterative approach with an increasing spatial resolution of vectors is used in the start-up estimation. If a previous vector field is available then it is applied as an initial guess.

Several methods for estimating the actual displacement (see Figure 6) were tested, such as 2D standard deviation, 2D correlation coefficient and root mean square error, which all yielded similar results. The 2D correlation coefficient was opted for. The retrieved vectors are estimated in the minimisation of a cost function that is

weighted between the "raw" displacement and the smoothness. Depending on the weighting, the retrieved vectors are generally smooth (non-divergent/convergent).

The methodology was tested on synthetic data and the result from a perfect rotation of 5 degrees and the same rotation with a translation is illustrated in Figure 10.
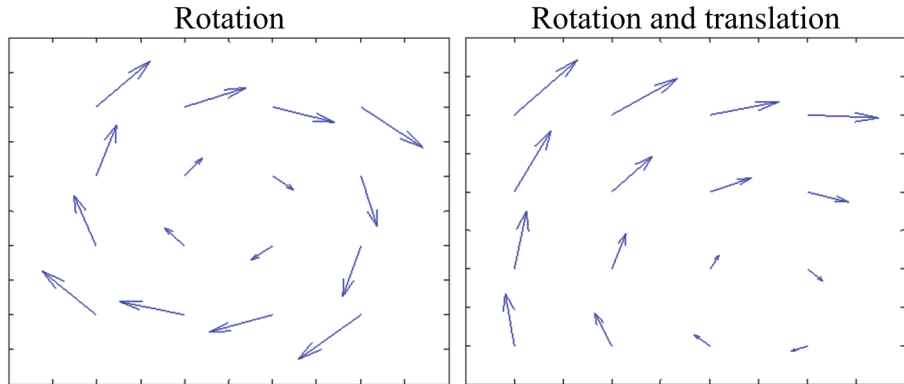

Figure 10: Example of advection field estimation of synthetic data of a rotation and rotation and translation (Technical Note I).

As illustrated in Figure 10, the methodology is capable of predicting the expected motion. Since the data was artificial generated was the displacement known. The estimated motion was perfect in translation scenarios but minor discrepancies was found in rotational scenarios (rotation and rotation combined with translation).

Tests on real data gave likewise promising results. The advantage is that, depending on the settings for the weights, the flow pattern of the advection field will always be smooth and indeed the overall flow pattern will be estimated. This estimate is only slightly affected by the growth and decay at small scale. This is the strength of the methodology.

The computation time for vector retrieval in real-time applications cannot take more than a several seconds. If the estimation is too computationally heavy then the result is that the prediction is not available in time for further processing.

Depending on the number of vectors needed, this methodology, at its current development stage, will take up to several minutes and can therefore not be applied in real-time applications. However, it should be possible to optimise on the minimisation part to yield results faster.

A thorough comparison should be conducted in order to determine whether or not the new method leads to a better performance than Co-TREC. Objectively, the new

method could be expected to be more stable than standard Co-TREC without Kalman filtering.

The difference between the two is that the new method is constrained in how much each vector can directly deviate from the surrounding vectors, whereas Co-TREC imposes continuity on the (free-flow) boundaries and not the individual vector. The result is two different advection fields. The new methods advection field estimation will be more the overall flow pattern compared to Co-TREC that allows more variation between the individual vectors. On urban scales, the Co-TREC methodology is preferable since small scale variations are possible.

For these reasons, Co-TREC is still the preferred methodology for the remaining work of this Ph.D. study.

4.3. PAPER II: ASSIMILATION OF RADAR-BASED NOWCAST INTO A HIRLAM NWP MODEL

The core of the HydroCast project is data assimilation of both development and testing of assimilation techniques. The HydroCast project operates across several fields from hydrological forecasting, both short-term and long term but also precipitation nowcasting. The following describes how data assimilation is used within the current Ph.D. study to increase the accuracy of short term precipitation prediction (<6h).

The prospect for combining the predictions of REM and NWP is promising as conceptualised in Figure 2. Figure 2 demonstrates the quality of the forecasts based on three sources, extrapolation of current weather (REM), mesoscale NWP model and synoptic scale NWP model with model output statistics.

This conceptualisation after Browning (1980), focusing on REM and mesoscale NWP models, still applies today. This is demonstrated by Bowler, Seed et al. (2006) and Berenguer, Surcel et al. (2012) who found that REM outperform mesoscale NWP models (hereafter NWP models) for lead-times up to 4 hours.

Several methods for combining REM with NWP predictions, hereby utilising the strengths of each method, have been proposed. One method applied in STEPS, described in section 3.2, combines the different spectral scales by weighting the cascades from REM and NWP as a function of skill. In general, most methods are based on some kind of weighting to combine the different predictions. Another approach is the possibility to assimilate the REM prediction into the NWP model. The only study on this subject, prior to the work of *Paper II*, was performed by Sokol, Zacharov (2012) who found using a water vapour correction method produced a slight improvement in the first hour but a significant improvement in performance of the second and third hour lead-time from the assimilation. The

major advantage of assimilation, compared to combining, is that the two predictions will never be different to a degree that makes seamless blending impossible. Furthermore, the NWP is forced into what is believed to be a more correct state, which also has the possibility to yield improvements on longer lead-times than within the assimilation window.

The work of *Paper II* was conducted in close cooperation with the Centre for Meteorological Models at the Research and Development Department, DMI. The study uses an assimilation technique introduced as a nudging scheme described by Korsholm, Petersen et al. (2014), developed at DMI. The radar derived QPE is nudged into the DMI HIRLAM NWP model by enhancing convection in the case of under-prediction and reducing convection in the opposite case. This is achieved by adding a nudging term to the divergence in the mass continuity equation. The methodology has some similarities to latent heat nudging (Jones, Macpherson 1997) but must be considered a more direct approach (Korsholm, Petersen et al. 2014). The REM data is produced by the Co-TREC based model with temporal Kalman filtering as described previously.

Eight events from August 2010 including a single case from 2 July 2011 were evaluated to test the new nudging assimilation of REM data. A reference nowcast was run to estimate the impact of the REM assimilation. The reference run and the run assimilated with REM uses the same initial analysis. 3D-var is used to assimilate surface observations, satellite data, radiosondes and aircraft data, which in the variational approach are used to correct the 3D fields of temperature, humidity and wind using a cut-off of 120 min. Furthermore, in the analysis, observed radar QPE and satellite cloud observations are assimilated using the methodology of (Korsholm, Petersen et al. 2014). The only difference between the two runs is the assimilation of the REM data.

The verification method to evaluate the impact of the REM assimilation in HIRLAM NWP model is the fractional skill score (FSS) derived by Roberts, Lean (2008). FSS is a spatial verification method that evaluates at which spatial scale the nowcast has skill. The verification method is based on comparing observed and nowcasted logical fractions within an increasing size of boxes (spatial scale) based on thresholding.

The results from comparing the reference run and the assimilated run of the nine events are very clear. It shows a large difference in performance by nudging REM data into HIRLAM NWP model in favour of assimilating REM data. The improvement is demonstrated for all nine events see Figure 11.
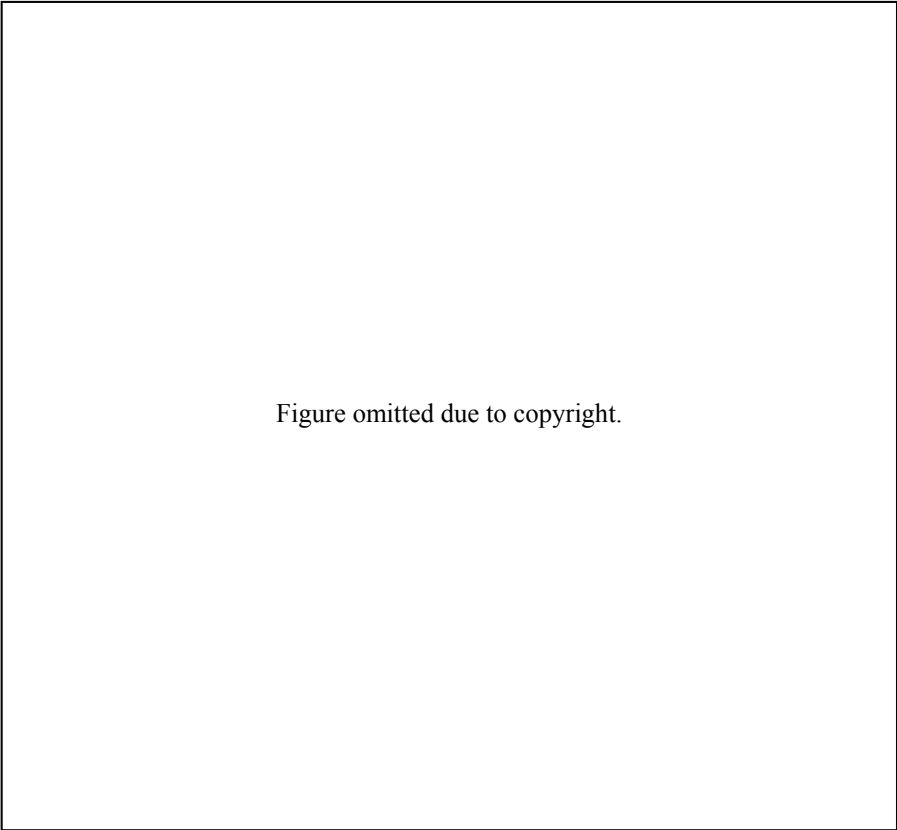
Figure omitted due to copyright.

Figure 11: The spatial scale at which the nowcast is skilled. The red line is the prediction with radar extrapolation data (RED) assimilated and the blue line is the prediction with no RED assimilated. The vertical lines indicates the start and end of assimilation of RED (lead-time 0-120 min). (Jensen, Petersen et al. 2014)

The case from 2 July 2011 was an especially intensive event that caused severe flooding of Copenhagen (see Figure 1), Denmark, as previously mentioned. The accumulated predicted precipitation of the reference run from the 2 most critical hours gave $30 - 60\ mm$ in the Copenhagen area whereas the REM assimilated prediction was $75 - 150\ mm$. The actual observed precipitation from radar QPE was $75 - 150\ mm$. However, slightly less widespread as predicted by the REM assimilated run. The accumulated precipitation covering the area of Copenhagen is illustrated in Figure 12.

Figure omitted due to copyright.

Figure 12: Accumulated precipitation from the 2ⁿᵈ July 2011 from 1200 to 1400 UTC. (Jensen, Petersen et al. 2014). Where RED is the radar extrapolation data.

Another important aspect of the assimilation is that the improvement is not only obtained in the assimilation period but also afterwards. This is one of the major advantages of using assimilation compared to combining techniques.

Presently the method is being developed into an operational system at Centre for Meteorological Models at the Research and Development Department, Danish Meteorological Institute (DMI). This involves development of a REM and high quality control of the radar derived QPE product. It is highly important that noise and other types of uncertainty is minimised in the data prior to assimilation.

4.4. SUMMARY

The first part of the Ph.D. study focuses on improving the deterministic part of nowcasting. It was chosen to work with temporal stabilising of the advection field based on a developed Co-TREC model since noisy fluctuations over time were observed. On average, no improvement in performance could be detected. However, the stability in performance was improved which is important for the applicability of the prognosis. A new methodology for vector retrieval was developed that seems very promising but the computational time at the given development stage needs to be improved for real-time applications. Lastly, a new methodology for utilising the best from REM and NWP predictions was developed. The assimilation approach was found, for nine events, to highly improve the quality of the assimilated NWP prognosis and is now underway to be implemented operationally at DMI.

CHAPTER 5. DEVELOPMENT OF PROBABILISTIC QUANTITATIVE UNCERTAINTY ESTIMATION METHODS

The focus of the first part of the Ph.D. study was to improve the deterministic part of REM (model error) and how to assimilate REM data into NWP predictions. As mentioned previously, the deterministic part is a basis for the probabilistic approach and it is therefore important to ensure stability and to give the best possible prediction prior to developing probabilistic predictions. The second part addresses the uncertainties of nowcasting by probabilistic approaches. This is done to give better possibilities for decision-making in the context of RTC of urban drainage systems.

5.1. PAPER III: ENSEMBLE PREDICTION SYSTEM BASED ON LAGRANGIAN EXTRAPOLATION OF RADAR DERIVED PRECIPITATION (RESEMBLE)

The work of *Paper III* addresses the uncertainties of REM nowcasting. It is based on the ensemble approach for the applicability in hydrological models. Ensemble members can, as described previously, be directly used in hydrological modelling since they are temporally and spatially correlated.

The developed ensemble prediction system (RESEMBLE) separates the advection uncertainty from the growth and decay uncertainty. Error models for each source were developed and used to generate ensemble members whose spread describes the combined uncertainty of the nowcast.

The objective for the new ensemble prediction system is to develop a methodology which is very computationally efficient and can be applied in real-time applications. The novelty of the approach lies in the way the uncertainty is estimated by separating the sources and the way the temporal correlation is imposed.

The approach is based on estimation of error models from historical deterministic nowcasts compared to observation radar data performed offline. The error models is separated into the following three:

- Advection uncertainty
- Cell uncertainty
- Non-cell uncertainty (the spurious intensities)

The statistics of the error models originates from comparing historical nowcasted data with observations from the years 2011 and 2012. The nowcasted data is based on the previously described Co-TREC model with temporal Kalman filtering.

The sequence of generating the ensemble members is as follows:

1. Generate the deterministic nowcast (with a temporal discretisation based on an estimated cell lifetime (60 min))
2. Generate ensemble members based on perturbations in the advection field
3. Identify cells (areas of interest) in each ensemble member
4. Generate perturbation of the cells
5. Generate perturbations of the precipitation not covered by the cells.
6. Interpolate across lead-time to obtain the wanted temporal resolution of the nowcast and to ensure the temporal correlation.

The error model for advection uncertainty is estimated from the advection error estimated by 2D normalised cross correlation (Lewis 1995); very similar to the approach by Schmid, Mecklenburg et al. (2000). Since the historical advection error was shown to be both linear as a function of lead-time and Gaussian in x- and y-direction, the advection field is perturbed with a disturbance drawn from a two-dimensional Gaussian distribution based on the historical statistics. The perturbation is added to the advection field as described in equation (18).

$$\widehat{\psi_n}(t_0 + \tau, \boldsymbol{x}) = \psi\big(t_0, \boldsymbol{x} - (\boldsymbol{\alpha} + \boldsymbol{\delta_n})\big) \tag{18},$$

where ψ is the observed precipitation field, t_0 is the issue time of the nowcast, τ is the lead-time, $\boldsymbol{x}$ is the position, $\boldsymbol{\alpha}$ is the displacement vector (advection field), $\boldsymbol{\delta_n}$ is the advection perturbation for ensemble nowcast n and $\widehat{\psi_n}$ is the nowcasted precipitation field for ensemble nowcast n.

The error model for the cell uncertainty is based on the LU decomposition algorithm also applied in the model of REAL developed by Germann, Berenguer et al. (2009) but without the temporal correlation. At this juncture it should be noted that cells should not be thought of as convective storm cells but more as areas of interest. The cell-space-error statistics are computed by comparing observed and nowcasted cells. Since the advection error is addressed separately, the displacement error between the two compared cells is minimised as much as possible. This is done by aligning the cells according to the estimated displacement as the advection error using 2D normalised cross correlation. The error statistics (space structure of error) is in form of the mean error and covariance matrix of the residual error. The

cell perturbations, to be added the nowcast, is generated using Gaussian random white noise and the LU decomposition algorithm.

The last part of the nowcasted precipitation that is not covered by the cells also needs to be perturbed. The approach for estimation of the error model is fairly simple. Again observations and nowcasts are compared without the cell areas. The error standard deviation and mean error is computed as an average across lead-time from historical data. A perturbation is then generated by multiplying white noise with the found standard deviation and adding the mean error. This perturbation is then added to the areas not covered by the cells scaled with lead-time so it has full effect at the longest lead-time.

If each lead-time step (i.e. 10 minutes) of the deterministic nowcast was to be perturbed, the uncertainty of growth and decay would be uncorrelated in time and overestimated. Instead, the average cell lifetime is estimated following the lifetime definition of Germann, Zawadzki (2002). The aligned cells from the two years of data were found to have an average lifetime of 62 min and so for these reasons the 60 min and 120 min lead-time of the deterministic nowcast are perturbed and only the 60 min and 120 min.

The last step in the ensemble nowcasts generation is therefore to fill out the missing predictions in between observation and the perturbed 60 min and 120 min lead-time. The assumption is that the transformation from one image to the next (60 minutes) is linear. This is achieved by temporal interpolation between images following the methodology developed by Nielsen, Thorndahl et al. (2014). This ensures a natural transition from observation to prediction and temporal correlation.

Figure 13 shows an example of two ensemble members from lead-times of 10 min, 60 min and 120 min along with the deterministic nowcast and observation from 08th July 2011.

The skill scores used to verify the ensemble prediction system shows that ensemble mean has a higher 2D correlation coefficient than the deterministic nowcast. The ensemble spread is in proportion with the uncertainty and the ensemble members are able to predict the location of precipitation for thresholds of $0.1 \frac{mm}{hr}$, $1 \frac{mm}{hr}$, $2.5 \frac{mm}{hr}$ and for most events also $5 \frac{mm}{hr}$ with skill in the full range up to 120 min lead-time.

The ensemble generation is very computational efficient and the generation of 100 ensemble nowcasts takes less than 30 seconds on a standard computer, without parallelisation. This makes it applicable to real-time hydrological forecasting such as RTC of the urban drainage system. To study of the ensemble prediction system is able to reasonably predict the precipitation for up to 60 min lead-time. The

ensemble prognosis is used as input for the urban drainage system for the city of Frejlev.
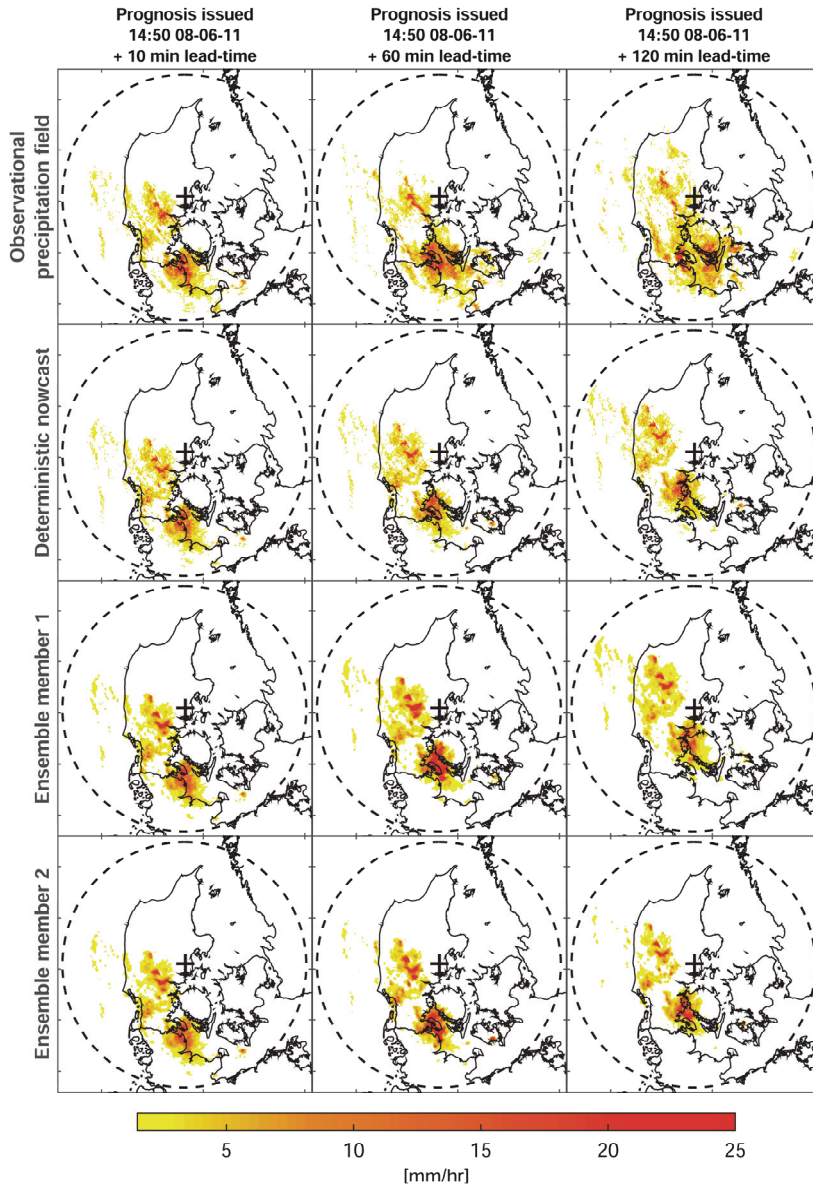

Figure 13: Examples of 2 ensemble members, deterministic nowcast and observations for lead-time 10 min, 60 min and 120 min. The plots depict the precipitation field from a minimum threshold of 0.5 mm/hr.

5.2. PAPER IV: ENSEMBLE PREDICTION OF FLOW IN URBAN DRAINAGE SYSTEMS USING RESEMBLE

Ensemble nowcasts for 22 events with a new prognosis every 10 min and 300 ensemble members were generated and used as input for the urban drainage system of Frejlev.

Frejlev is a small city covered by only 3 radar pixels with a spatial resolution of 2000x2000 m. With only few pixels covering the catchment, the demand for the prediction is high since there is very low response time in the system. This means that even small discrepancies in the prognosis and observations will give either large residual errors or offsets. For larger catchments this is not as critical since the errors will be distributed over a larger area and "smoothened". Furthermore, the spatial predictability is even more critical since even small displacements would lead to wrong predictions. The catchment of Frejlev can be seen in Figure 14.
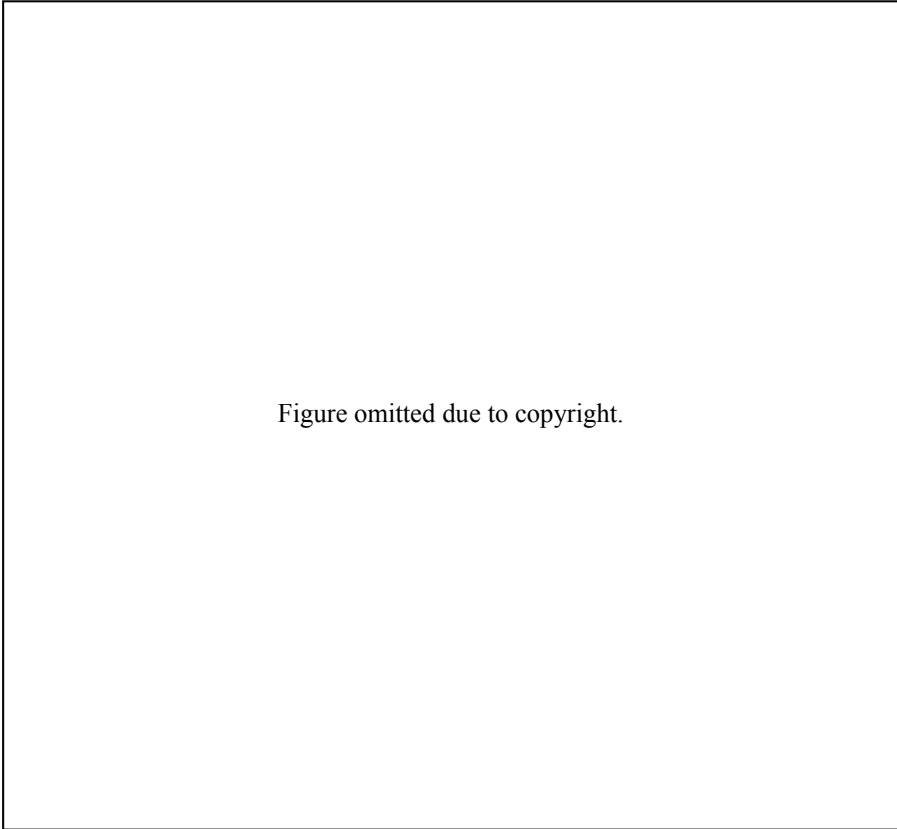
Figure 14: The urban drainage system of Frejlev and the three radar pixels covering the catchment. (Jensen, Thorndahl et al. 2015)

The drainage system is simulated in the Mike Urban 2013 software as a fully distributed model. The runoff is based on a time-area surface runoff sub model combined with a pipe flow sub model described by the 1D Saint-Venant equations.

Figure 15 shows an example of the input, from event 8, to the urban drainage model from one of the three pixels covering the catchment. For this event the ensemble prediction is good at encapsulating the uncertainty of the nowcast for all three lead-times. It can also be observed that the ensemble members follow the deterministic nowcast, which also underlines the importance for precise deterministic nowcasts. The output from the urban drainage model using the input from Figure 15 can be seen in Figure 16. The simulated response is well predicted.

Figure omitted due to copyright.

Figure 15: Time series of rainfall from one of the pixels over Frejlev. The figure illustrates the 95 % confidence interval of the ensemble, ensemble mean, and deterministic nowcast against the observed radar rainfall. (Jensen, Thorndahl et al. 2015)
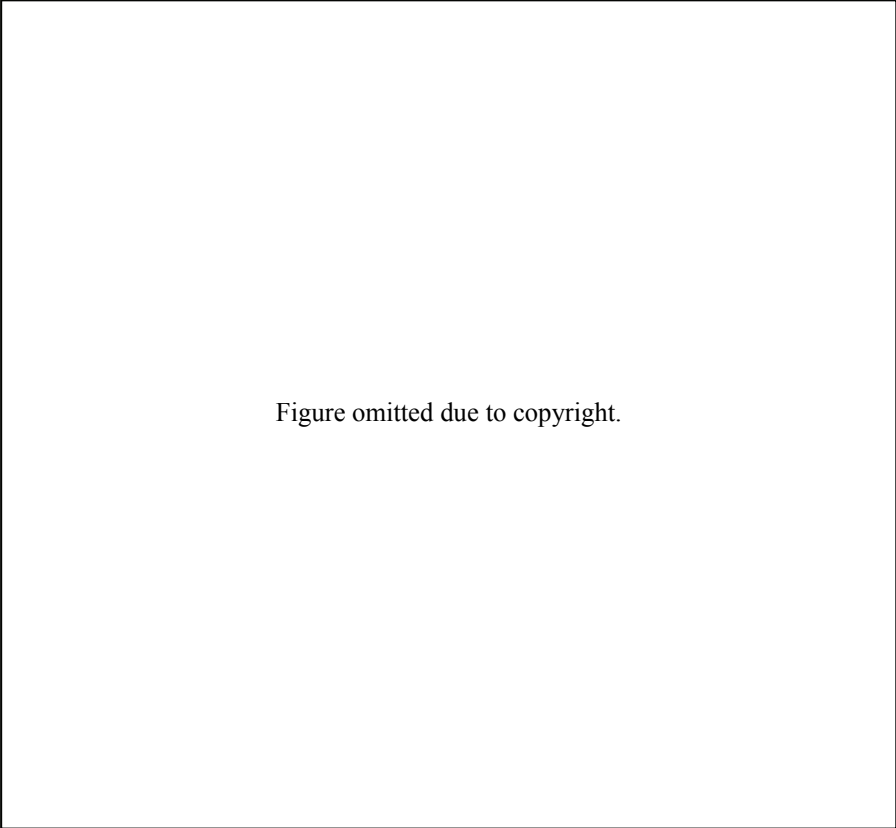
Figure omitted due to copyright.

Figure 16: Predicted flow in event 8 from ensemble and deterministic nowcasts compared to observed radar rainfall for 10, 30 and 60 min lead times. (Jensen, Thorndahl et al. 2015)

The simulated responses from all of the 22 events was evaluated with respect to the runoff volume, volume of combined sewer overflow, time to centre of volume (eccentricity/offset) and peak flow compared with simulated responses from observational radar input. In general the results are encouraging. Most of the events are well simulated and the uncertainty is described by the spread of the ensemble nowcasts.

This also implies that there is a potential for real-time control of the urban drainage system following the methodology of the developed REM ensemble prediction system. The results originate from a very small catchment with very short response times which also justifies the short lead-times of the ensemble nowcast. For larger catchments, longer lead-times would be needed due to the longer response times. This is especially true if the objective is RTC. Extending the lead-time is not

possible with extrapolation models since the maximum lead-time is determined by, among other things, the range of the radar, however this could be possible with larger mosaics. The following work studies the possibility for ensemble generation by assimilation of REM predictions into HIRLAM NWP model to achieve that extra lead-time.

5.3. PAPER V: ASSIMILATION OF ENSEMBLE RADAR BASED NOWCAST INTO HIRLAM NWP MODEL FOR HIGH INTENSITY RAINFALL ESTIMATION

Normally ensemble members from NWP models are initiated by introducing disturbances in the initial conditions (IC) and/or lateral boundary conditions (LBC). For nowcasting can this lead to some problems with not generating effective members from the beginning. In other words, disturbances in the IC or LBC takes time to generate the wanted spread of the ensemble members. For nowcasting and urban drainage applications, this is not optimal.

The idea of the study is to demonstrate that it is possible to generate NWP ensemble members by assimilation of REM ensemble members and furthermore utilise the pronounced improvements in performance when assimilating REM data as demonstrated in sub-section 4.3. In theory, this would result in ensemble nowcasts whose spread describes the uncertainty but still has the performance equal to REM nowcasts for short lead-times combined with the advantages of the NWP models source/sink terms for better predictability of longer lead-times.

The methodology starts by generating 100 REM ensemble nowcasts, using the model described in section 5.1, and selects 25 that have an equal spread around the deterministic nowcast estimated by the 2D standard deviation. This is done in order to represent the uncertainty since 25 random ensemble members could lead to 25 very similar predictions. The specific number 25 is chosen due to practical considerations regarding computational time of HIRLAM NWP model.

The DMI HIRLAM NWP model is then run 25 times, with the same initial analysis as described in sub-section 4.3, and with continuous assimilation of the REM nowcast ensemble members. The combined system is called HIRLAM ensemble prediction system (H-EPS). The assimilation method follows the nudging technique developed by Korsholm, Petersen et al. (2014).

In total eight events from August 2010 were processed - the same events from *Paper II* described in section 4.3. In Figure 17, an example of one ensemble member is seen along with observed radar data at lead-time 380 min from three events. Furthermore, two ensemble members are enlarged to show the difference in predictions.
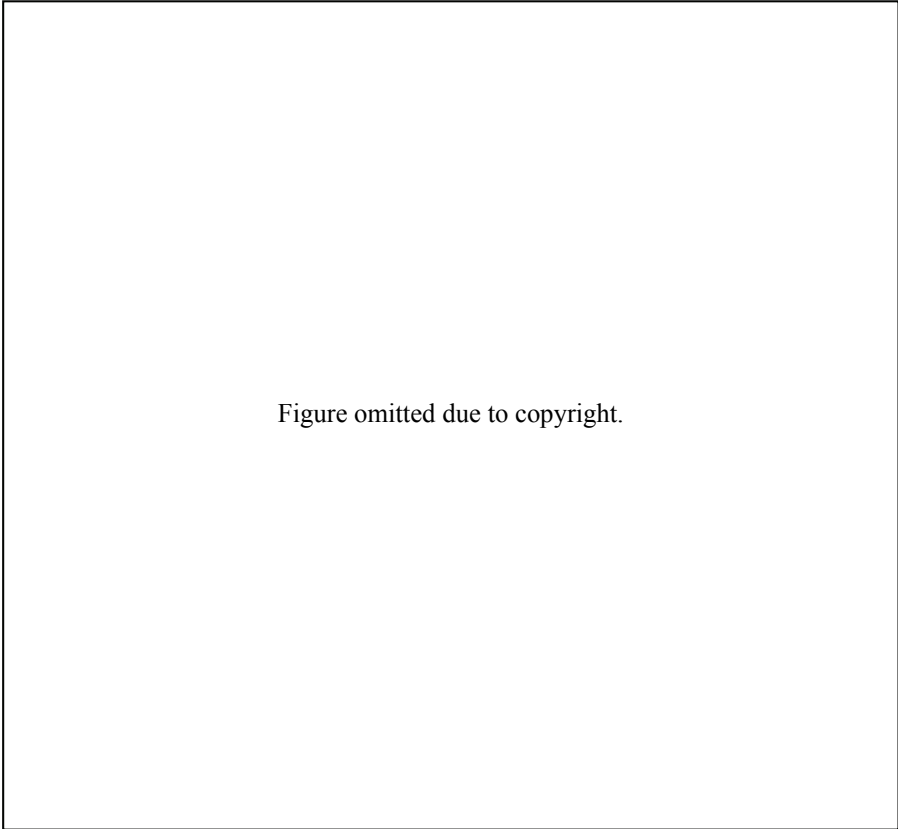
Figure omitted due to copyright.

Figure 17: The plots depicts radar observation, ensemble mean and two zoomed in ensemble members for event 2, event 7 and event 8 with a lead-time of 6 h and 20 min. The plots depict the precipitation field from a minimum threshold of 0.5 mm/hr. (Jensen, Petersen et al. 2015)

Taking the lead-time into account, the predictions are very good. The larger scales of the precipitation and the overall location is well predicted. This is the case for all of the eight events.

The skill of H-EPS ensemble mean is compared, by 2D correlation coefficient, to two reference runs. Reference run 1 is with an initial analysis that did not assimilate radar QPE in the spin-up period as opposed to reference run 2 where radar QPE is assimilated. Reference run 2 and the ensemble members therefore have the exact same initial analysis. For all events, the ensemble mean performs better than both of the reference runs, despite the fact that ensemble mean will always smoothen both high and low intensity precipitation. In general the ensemble mean is not optimal in a prediction optimised toward high intensity precipitation.

Estimating the skill of the ensemble members using receiver operating characteristic area under curve (ROC AUC) from four thresholds of $0.1 \frac{mm}{hr}$, $1 \frac{mm}{hr}$, $2.5 \frac{mm}{hr}$ and $5 \frac{mm}{hr}$ reveals high skill. For several of the events, random skill is not reached for any of the thresholds. This is quite impressive considering the lead-times of up to 380 min.

The results shows a bias towards to high intensities especially in the first half of the nowcast which is not coincidental. It was chosen to make H-EPS tuned towards high intensity rainfall with the focus to estimate the probability for decision makers. Probability maps are developed in order to make an easy and visual way to simplify the probability. An example of this can be seen in Figure 18.

The results seem quite convincing when taking the long lead-time into account. The location is well predicted along with the probabilities. For event 8 there is a tendency of overestimation of the rainfall to the west but both of the other cases are well predicted. The three examples shown are not exceptional but similar results for the remaining cases are observed.

Three things can be concluded from the study. The first thing is that it is possible to generate NWP ensemble members by assimilation of REM ensemble members that is initiated immediately. Secondly that the skill of the NWP prediction is improved by the assimilation which is not only limited to the assimilation period. Thirdly, the developed probability maps are able to indicate the location of intense precipitation. That H-EPS is fairly adept in predicting the location of high intensity precipitation and is very useful in the context of RTC of urban drainage systems.

Figure omitted due to copyright.

Figure 18: Probability map from event 2, event 7 and event 8 of 1h-accumulated precipitation along with the observed precipitation above 5 mm/hr. The probability map is computed from accumulated precipitation from the 6th hour to the 7th hour lead-time. (Jensen, Petersen et al. 2015)

5.4. SUMMARY

The second part of the Ph.D. study focuses on addressing the uncertainties of deterministic nowcasting. A new REM ensemble prediction methodology is developed with the focus of being computationally efficient so it is applicable to real-time hydrological forecasting. The novelty of the new methodology lies in the way the uncertainty is estimated by separating the error sources and the way the temporal correlation is imposed. The REM ensemble predictions were used as input in a simulation for a small urban catchment to test the accuracy of the probabilistic predictions in the context of urban drainage applications. The results were promising for most of the 22 tested events, which indicates possibilities for RTC of drainage systems using the REM ensemble prediction system. Lastly, a new methodology for generation of NWP ensemble members by assimilation of REM ensemble members was developed. The results are very promising and display high skill for both short and long lead-times. The method makes it possible to combine the high skill of REM for short lead-times with the better predictability of NWP for longer lead-times cf. Figure 2. The ensemble members are initiated quickly which is needed if the application for the prediction is short-term hydrological forecasting.

CHAPTER 6. CONCLUSION

The main purpose of this Ph.D. study is to enhance nowcasting of 0-6 hour lead-time for increased applicability in RTC of urban drainage systems. A precursor of this was to try to improve the precision of the deterministic Co-TREC based REM nowcast.

Improvements to the spatial precision were attempted by temporal filtering of the advection field since flickering or noise was observed over time. A Kalman filter was calibrated against observed Doppler velocities to obtain realistic behaviours and was implemented for exactly this purpose. Although the results showed only a slight improvement in skill, a major increase in stability was demonstrated.

The evolution of precipitation at urban scales is extremely difficult to predict. It was therefore chosen not to try to deterministically improve the evolution precision of the REM prediction but instead to take a probabilistic approach. A new methodology, called RESEMBLE, which is very computationally efficient was developed to describe the nowcast uncertainty. The uncertainty of the prediction is expressed as a set of ensemble members whose spread determines the uncertainty. Ensemble members also have the advantage that they are directly applicable in urban drainage modelling. RESEMBLE's novelty lies in the way the temporal correlation is applied and in the way that the uncertainty sources of evolution/decay and advection uncertainty are separated. The temporal correlation is imposed by a numeric interpolation method. RESEMBLE was tested as input in the urban drainage model of Frejlev, Denmark. Compared to observational radar QPE as input did the prediction perform well up to 60 min. for most tested events.

The quality of a REM prediction at urban scales deteriorates rapidly due to the frozen initial condition. To extend lead-time it has been proven, as one of the major scientific contributions of this Ph.D. study, that assimilation of deterministic REM data into the HIRLAM NWP model improves NWP predictability. Not only is the improvement notable in the assimilation period, but it continues to have a positive effect on the prediction post-assimilation. It was demonstrated that the aforementioned flood of the Copenhagen area the 2nd July 2011 could have been much more precisely predicted using this assimilation approach and possible warnings could have been issued earlier than was the case.

Lastly, it has been demonstrated that it is possible to initiate NWP ensemble members by assimilation of REM ensemble members, which are initiated immediately. This method combines the two prediction methodologies and utilises each of their strengths by nudging the atmospheric state of the NWP model towards a more correct state. This also improves predictability beyond the assimilation

period. Again, the ensemble members are directly applicable for hydrological modelling.

In conclusion, based on the above described results, it is possible to improve stability and extend lead-time by assimilation techniques, whereby the strengths of these techniques complement each other. The results also imply that it is possible to describe the uncertainty of nowcasts which are applicable for RTC. This gives overall a better basis for RTC of urban drainage systems. Methods have been developed that operate on both very short lead-time, often sufficient for small catchments, and for longer lead-times up to 380 min, which is needed for larger catchments.

BIBLIOGRAFY

ANDERSSON, T. and IVARSSON, K., 1991. A model for probability nowcasts of accumulated precipitation using radar. *Journal of Applied Meteorology,* **30**(1), pp. 135-141.

ATENCIA, A. and ZAWADZKI, I., 2014. A Comparison of Two Techniques for Generating Nowcasting Ensembles. Part I: Lagrangian Ensemble Technique. *Monthly Weather Review,* **142**(11), pp. 4036-4052.

AUSTIN, G. and BELLON, A., 1974. The use of digital weather radar records for short-term precipitation forecasting. *Quarterly Journal of the Royal Meteorological Society,* **100**(426), pp. 658-664.

AYDIN, K., ZHAO, Y. and SELIGA, T., 1989. Rain-induced attenuation effects on C-band dual-polarization meteorological radars. *Geoscience and Remote Sensing, IEEE Transactions on,* **27**(1), pp. 57-66.

BALLY, J., 2004. The Thunderstorm Interactive Forecast System: Turning automated thunderstorm tracks into severe weather warnings. *Weather and forecasting,* **19**(1), pp. 64-72.

BATTAN, L.J., 1959. *Radar meteorology.* Chicago: University of Chicago Press.

BATTAN, L.J., 1973. Radar observation of the atmosphere.

BERENGUER, M., SEMPERE-TORRES, D. and PEGRAM, G., 2011. SBMcast–An ensemble nowcasting technique to assess the uncertainty in rainfall forecasts by Lagrangian extrapolation. *Journal of Hydrology,* **404**(3), pp. 226-240.

BERENGUER, M., SURCEL, M., ZAWADZKI, I., XUE, M. and KONG, F., 2012. The diurnal cycle of precipitation from continental radar mosaics and numerical weather prediction models. Part II: Intercomparison among numerical models and with Nowcasting. *Monthly Weather Review,* **140**(8), pp. 2689-2705.

BOWLER, N.E., PIERCE, C.E. and SEED, A.W., 2006. STEPS: A probabilistic precipitation forecasting scheme which merges an extrapolation nowcast with downscaled NWP. *Quarterly Journal of the Royal Meteorological Society,* **132**(620), pp. 2127-2155.

BOWLER, N.E., PIERCE, C.E. and SEED, A., 2004. Development of a precipitation nowcasting algorithm based upon optical flow techniques. *Journal of Hydrology,* **288**(1), pp. 74-91.

BRINGI, V.N., KEENAN, T. and CHANDRASEKAR, V., 2001. Correcting C-band radar reflectivity and differential reflectivity data for rain attenuation: A self-consistent method with constraints. *Geoscience and Remote Sensing, IEEE Transactions on,* **39**(9), pp. 1906-1915.

BROWNING, K., 1980. Review lecture: local weather forecasting, *Proceedings of the Royal Society of London A: Mathematical, Physical and Engineering Sciences* 1980, The Royal Society, pp. 179-211.

CAO, Q., HONG, Y., QI, Y., WEN, Y., ZHANG, J., GOURLEY, J.J. and LIAO, L., 2013. Empirical conversion of the vertical profile of reflectivity from Ku-band to S-band frequency. *Journal of Geophysical Research: Atmospheres,* **118**(4), pp. 1814-1825.

CHRISTENSEN, J.H., ARNBJERG-NIELSEN, K., GRINDSTED, A., HALSNÆS, K., JEPPESEN, E., MADSEN, H., OLESEN, J.E., PORTER, J.R., REFSGAARD, J.C. and OLESEN, M., 2014. *Analyse af IPCC delrapport 2 - Effekter, klimatilpasning og sårbarhed.*

COLLIER, C., 1986. Accuracy of rainfall estimates by radar, Part I: Calibration by telemetering rain gauges. *Journal of Hydrology,* **83**(3), pp. 207-223.

CRESSMAN, G.P., 1959. An operational objective analysis system. *Monthly Weather Review,* **87**(10), pp. 367-374.

DA SILVEIRA, R.B. and HOLT, A.R., 2001. An automatic identification of clutter and anomalous propagation in polarization-diversity weather radar data using neural networks. *Geoscience and Remote Sensing, IEEE Transactions on,* **39**(8), pp. 1777-1788.

DIXON, M. and WIENER, G., 1993. TITAN: Thunderstorm identification, tracking, analysis, and nowcasting-A radar-based methodology. *Journal of Atmospheric and Oceanic Technology,* **10**(6), pp. 785-797.

DOELLING, I.G., JOSS, J. and RIEDL, J., 1998. Systematic variations of Z-R-relationships from drop size distributions measured in northern Germany during seven years. *Atmospheric Research,* **47-48**, pp. 635-649.

GABELLA, M. and NOTARPIETRO, R., 2002. Ground clutter characterization and elimination in mountainous terrain, *Proceedings of ERAD* 2002.

GERMANN, U., BERENGUER, M., SEMPERE-TORRES, D. and ZAPPA, M., 2009. REAL—Ensemble radar precipitation estimation for hydrology in a

mountainous region. *Quarterly Journal of the Royal Meteorological Society,* **135**(639), pp. 445-456.

GERMANN, U., GALLI, G., BOSCACCI, M. and BOLLIGER, M., 2006. Radar precipitation measurement in a mountainous region. *Quarterly Journal of the Royal Meteorological Society,* **132**(618), pp. 1669-1692.

GERMANN, U. and ZAWADZKI, I., 2004. Scale dependence of the predictability of precipitation from continental radar images. Part II: Probability forecasts. *Journal of Applied Meteorology,* **43**(1), pp. 74-89.

GERMANN, U. and ZAWADZKI, I., 2002. Scale-dependence of the predictability of precipitation from continental radar images. Part I: Description of the methodology. *Monthly Weather Review,* **130**(12), pp. 2859-2873.

GERMANN, U., ZAWADZKI, I. and TURNER, B., 2006. Predictability of precipitation from continental radar images. Part IV: Limits to prediction. *Journal of the Atmospheric Sciences,* **63**(8), pp. 2092-2108.

GOLDING, B.W., 1998. *Nimrod: A system for generating automated very short range forecast.*

GOURLEY, J.J., GIANGRANDE, S.E., HONG, Y., FLAMIG, Z.L., SCHUUR, T. and VRUGT, J.A., 2010. Impacts of polarimetric radar observations on hydrologic simulation. *Journal of Hydrometeorology,* **11**(3), pp. 781-796.

GRAY, W., UDDSTROM, M. and LARSEN, H., 2002. Radar surface rainfall estimates using a typical shape function approach to correct for the variations in the vertical profile of reflectivity. *International Journal of Remote Sensing,* **23**(12), pp. 2489-2504.

HARRISON, D., DRISCOLL, S. and KITCHEN, M., 2000. Improving precipitation estimates from weather radar using quality control and correction techniques. *Meteorological Applications,* **7**(02), pp. 135-144.

HORN, B.K. and SCHUNCK, B.G., 1981. Determining optical flow, *1981 Technical symposium east* 1981, International Society for Optics and Photonics, pp. 319-331.

HWANG, P.Y. and BROWN, R.G., 1997. Introduction to random signals and applied Kalman filtering. *John Wiley & Sons, Inc.,* **5**, pp. 39-45.

JENSEN, D.G., PETERSEN, C. and RASMUSSEN, M.R., 2015. Assimilation of ensemble radar based nowcast into HIRLAM NWP model for high intensity rainfall estimation. *Awaiting publication*.

JENSEN, D.G., THORNDAHL, S. and RASMUSSEN, M.R., 2015. Ensemble prediction of flow in urban drainage systems using RESEMBLE. *Awaiting publication*.

JENSEN, D.G., PETERSEN, C. and RASMUSSEN, M.R., 2014. Assimilation of radar-based nowcast into a HIRLAM NWP model. *Meteorological Applications*.

JOE, P., FALLA, M., VAN RIJN, P., STAMADIANOS, L., FALLA, T., MAGOSSE, D., ING, L. and DOBSON, J., 2002. Radar data processing for severe weather in the national radar project of Canada. *SELS, San Antonio*, pp. 12-16.

JONES, C.D. and MACPHERSON, B., 1997. A latent heat nudging scheme for the assimilation of precipitation data into an operational mesoscale model. *Meteorological Applications,* **4**(3), pp. 269-277.

JOSS, J. and WALDVOGEL, A., 1970. A method to improve the accuracy of radar measured amounts of precipitation, *14th Conference on radar meteorology (preprints)* 1970, pp. 237-238.

JOSS, J., WALDVOGEL, A. and COLLIER, C., 1990. *Precipitation measurement and hydrology.* Springer.

KOISTINEN, J., 1991. Operational correction of radar rainfall errors due to the vertical reflectivity profile, *Preprints, 25th Int. Conf. on Radar Meteorology, Paris, France, Amer. Meteor. Soc.* 1991, pp. 91-94.

KORSHOLM, U.S., PETERSEN, C., SASS, B.H., NIELSEN, N.W., JENSEN, D.G., OLSEN, B.T., GILL, R. and VEDEL, H., 2014. A new approach for assimilation of 2D radar precipitation in a high-resolution NWP model. *Meteorological Applications*.

KRAJEWSKI, W.F., VIGNAL, B., SEO, B. and VILLARINI, G., 2011. Statistical model of the range-dependent error in radar-rainfall estimates due to the vertical profile of reflectivity. *Journal of Hydrology,* **402**(3), pp. 306-316.

KRÄMER, S., FUCHS, L. and VERWORN, H., 2007. Aspects of radar rainfall forecasts and their effectiveness for real time control-the example of the sewer system of the city of Vienna. *Water Practice and Technology,* **2**(2).

KRAWACK, S. and MADSEN, M.B., 2013. *Klimatilpasning – organisering og økonomi.* Concito.

LEE, G.W. and ZAWADZKI, I., 2005. Variability of drop size distributions: Time-scale dependence of the variability and its effects on rain estimation. *Journal of Applied Meteorology,* **44**(2), pp. 241-255.

LEWIS, J.P., 1995. Fast normalized cross-correlation, *Vision interface* 1995, pp. 120-123.

LI, P. and LAI, E.S., 2004. Short-range quantitative precipitation forecasting in Hong Kong. *Journal of Hydrology,* **288**(1), pp. 189-209.

LI, L., SCHMID, W. and JOSS, J., 1995. Nowcasting of motion and growth of precipitation with radar over a complex orography. *Journal of Applied Meteorology,* **34**(6), pp. 1286-1300.

LORENZ, E.N., 1965. A study of the predictability of a 28-variable atmospheric model. *Tellus A,* **17**(3).

LÖWE, R., THORNDAHL, S., MIKKELSEN, P.S., RASMUSSEN, M.R. and MADSEN, H., 2014. Probabilistic online runoff forecasting for urban catchments using inputs from rain gauges as well as statically and dynamically adjusted weather radar. *Journal of Hydrology,* **512**, pp. 397-407.

MARSHALL, J.S. and PALMER, W.M.K., 1948. The distribution of raindrops with size. *Journal of Meteorology,* **5**(4), pp. 165-166.

MARSHALL, J., HITSCHFELD, W. and GUNN, K., 1955. Advances in radar weather. *Advances in Geophysics,* **2**, pp. 1.

MECKLENBURG, S., JOSS, J. and SCHMID, W., 2000. Improving the nowcasting of precipitation in an Alpine region with an enhanced radar echo tracking algorithm. *Journal of Hydrology,* **239**(1), pp. 46-68.

MUELLER, C., SAXEN, T., ROBERTS, R., WILSON, J., BETANCOURT, T., DETTLING, S., OIEN, N. and YEE, J., 2003. NCAR auto-nowcast system. *Weather and Forecasting,* **18**(4), pp. 545-561.

NIELSEN, J.E., THORNDAHL, S. and RASMUSSEN, M.R., 2014. A numerical method to generate high temporal resolution precipitation time series by combining weather radar measurements with a nowcast model. *Atmospheric Research,* **138**, pp. 1-12.

OGDEN, F., SHARIF, H., SENARATH, S., SMITH, J., BAECK, M. and RICHARDSON, J., 2000. Hydrologic analysis of the Fort Collins, Colorado, flash flood of 1997. *Journal of Hydrology,* **228**(1), pp. 82-100.

PACHAURI, R.K., ALLEN, M., BARROS, V., BROOME, J., CRAMER, W., CHRIST, R., CHURCH, J., CLARKE, L., DAHE, Q. and DASGUPTA, P., 2014. Climate Change 2014: Synthesis Report. Contribution of Working Groups I, II and III to the Fifth Assessment Report of the Intergovernmental Panel on Climate Change.

PEGRAM, G.G. and CLOTHIER, A.N., 2001a. Downscaling rain fields in space and time, using the String of Beads model in time series mode. *Hydrology and Earth System Sciences Discussions,* **5**(2), pp. 175-186.

PEGRAM, G. and CLOTHIER, A., 2001b. High resolution space–time modelling of rainfall: the "String of Beads" model. *Journal of Hydrology,* **241**(1), pp. 26-41.

PEURA, M. and HOHTI, H., 2004. Optical flow in radar images, *Proceedings of the Third European Conference on Radar Meteorology (ERAD), Visby, Sweden, 6-10 September 2004* 2004.

PEURA, M., KOISTINEN, J. and HOHTI, H., 2006. Quality information in processing weather radar data for varying user needs, *Proceedings of ERAD* 2006, pp. 563-566.

PFISTER, A. and CASSAR, A., 1999. Use and benefit of radar rainfall data in an urban real time control project. *Physics and Chemistry of the Earth, Part B: Hydrology, Oceans and Atmosphere,* **24**(8), pp. 903-908.

PIERCE, C., EBERT, E., SEED, A., SLEIGH, M., COLLIER, C., FOX, N., DONALDSON, N., WILSON, J., ROBERTS, R. and MUELLER, C., 2004. The nowcasting of precipitation during Sydney 2000: an appraisal of the QPF algorithms. *Weather and Forecasting,* **19**(1), pp. 7-21.

PIERCE, C.E., HARDAKER, P.J., COLLIER, C.G. and HAGGET, C.M., 2000. *Gandolf: A system for generating automated nowcasts of convective precipitation.*

PROBERT-JONES, J., 1962. The radar equation in meteorology. *Quarterly Journal of the Royal Meteorological Society,* **88**(378), pp. 485-495.

RADHAKRISHNA, B., ZAWADZKI, I. and FABRY, F., 2012. Predictability of precipitation from continental radar images. Part V: Growth and decay. *Journal of the Atmospheric Sciences,* **69**(11), pp. 3336-3349.

REYNIERS, M., 2008. *Quantitative precipitation forecasts based on radar observations: principles, algorithms and operational systems.* Publication scientifique et technique: Royal Meteorological Institute of Belgium.

RHINEHART, R., 1981. A pattern recognition technique for use with conventional weather radar to determine internal storm motions. *Atmos.Technol,* **13**, pp. 119-134.

RICHARDS, W. and CROZIER, C., 1983. Precipitation measurement with a C-band weather radar in southern Ontario. *Atmosphere-Ocean,* **21**(2), pp. 125-137.

RINEHART, R.E., 2010. *Radar for meteorologists.* Fifth edition edn. Rinehart Publications.

RINEHART, R. and GARVEY, E., 1978. Three-dimensional storm motion detection by conventional weather radar.

ROBERTS, N.M. and LEAN, H.W., 2008. Scale-selective verification of rainfall accumulations from high-resolution forecasts of convective events. *Monthly Weather Review,* **136**(1), pp. 78-97.

SCHMID, W., MECKLENBURG, S. and JOSS, J., 2000. Short-term risk forecasts of severe weather. *Physics and Chemistry of the Earth, Part B: Hydrology, Oceans and Atmosphere,* **25**(10), pp. 1335-1338.

SEED, A.W., PIERCE, C.E. and NORMAN, K., 2013. Formulation and evaluation of a scale decomposition-based stochastic precipitation nowcast scheme. *Water Resources Research,* **49**(10), pp. 6624-6641.

SEED, A., 2003. A dynamic and spatial scaling approach to advection forecasting. *Journal of Applied Meteorology,* **42**(3), pp. 381-388.

SEMPERE-TORRES, D., CORRAL, C., RASO, J. and MALGRAT, P., 1999. Use of weather radar for combined sewer overflows monitoring and control. *Journal of Environmental Engineering,* **125**(4), pp. 372-380.

SHERMAN, C.A., 1978. A mass-consistent model for wind fields over complex terrain. *Journal of Applied Meteorology,* **17**(3), pp. 312-319.

SMITH, J.A. and KRAJEWSKI, W.F., 1991. Estimation of the mean field bias of radar rainfall estimates. *Journal of Applied Meteorology,* **30**(4), pp. 397-412.

SMITH, P. and JOSS, J., 1997. Use of a fixed exponent in ''adjustable''Z-R relationships, *Preprints, 28th Conf. on Radar Meteorology, Austin, TX, Amer. Meteor. Soc.* 1997, pp. 254-255.

SOKOL, Z. and ZACHAROV, P., 2012. Nowcasting of precipitation by an NWP model using assimilation of extrapolated radar reflectivity. *Quarterly Journal of the Royal Meteorological Society,* **138**(665), pp. 1072-1082.

STANIFORTH, A. and CÔTÉ, J., 1991. Semi-Lagrangian integration schemes for atmospheric models-a review. *Monthly Weather Review,* **119**(9), pp. 2206-2223.

SUGIER, J., DU CHATELET, J.P., ROQUAIN, P. and SMITH, A., 2002. Detection and removal of clutter and anaprop in radar data using a statistical scheme based on echo fluctuation. *Proceedings of ERAD (2002),* , pp. 17-24.

SURCEL, M., ZAWADZKI, I. and YAU, M., 2015. A study on the scale dependence of the predictability of precipitation patterns. *Journal of the Atmospheric Sciences,* **72**(1), pp. 216-235.

THOMPSON, E.J., RUTLEDGE, S.A., DOLAN, B. and THURAI, M., 2015. Drop size distributions and radar observations of convective and stratiform rain over the equatorial Indian and West Pacific Oceans. *Journal of the Atmospheric Sciences,* (2015).

THORNDAHL, S., NIELSEN, J.E. and RASMUSSEN, M.R., 2014. Bias adjustment and advection interpolation of long-term high resolution radar rainfall series. *Journal of Hydrology,* **508**, pp. 214-226.

THORNDAHL, S. and RASMUSSEN, M.R., 2009. Challenges in X-band weather radar data calibration, *The International Workshop on Precipitation in Urban Areas* 2009, pp. 12-16.

TURNER, B.J., ZAWADZKI, I. and GERMANN, U., 2004. Predictability of precipitation from continental radar images. Part III: Operational nowcasting implementation (MAPLE). *Journal of Applied Meteorology,* **43**(2), pp. 231-248.

UIJLENHOET, R. and POMEROY, J., 2001. Raindrop size distributions and radar reflectivity - rain rate relationships for radar hydrology. *Hydrology and Earth System Sciences Discussions,* **5**(4), pp. 615-628.

UIJLENHOET, R., SMITH, J.A. and STEINER, M., 2003. The microphysical structure of extreme precipitation as inferred from ground-based raindrop spectra. *Journal of the Atmospheric Sciences,* **60**(10), pp. 1220-1238.

VENEZIANO, D., BRAS, R.L. and NIEMANN, J.D., 1996. Nonlinearity and self-similarity of rainfall in time and a stochastic model. *Journal of Geophysical Research: Atmospheres (1984–2012),* **101**(D21), pp. 26371-26392.

VENUGOPAL, V., FOUFOULA-GEORGIOU, E. and SAPOZHNIKOV, V., 1999. Evidence of dynamic scaling in space-time rainfall. *Journal of Geophysical Research: Atmospheres (1984–2012),* **104**(D24), pp. 31599-31610.

VILLARINI, G. and KRAJEWSKI, W.F., 2010. Review of the different sources of uncertainty in single polarization radar-based estimates of rainfall. *Surveys in Geophysics,* **31**(1), pp. 107-129.

VIVONI, E.R., ENTEKHABI, D. and HOFFMAN, R.N., 2007. Error propagation of radar rainfall nowcasting fields through a fully distributed flood forecasting model. *Journal of applied meteorology and climatology,* **46**(6), pp. 932-940.

WAHBA, G. and WENDELBERGER, J., 1980. Some new mathematical methods for variational objective analysis using splines and cross validation. *Monthly Weather Review,* **108**(8), pp. 1122-1143.

WANG, J., KEENAN, T., JOE, P., WILSON, J., LAI, L., LIANG, F., WANG, Y., EBERT, B., YE, Q., BALLY, J., SEED, A., CHEN, M., XUE, J. and CONWAY, B., 2009. *Overview of the Beijing 2008 Olympics Project. Part I: Forecast Demonstration Project.* World Weather Research Programme.

WERNER, M. and CRANSTON, M., 2009. Understanding the value of radar rainfall nowcasts in flood forecasting and warning in flashy catchments. *Meteorological Applications,* **16**(1), pp. 41-55.

WILSON, J.W., EBERT, E.E., SAXEN, T.R., ROBERTS, R.D., MUELLER, C.K., SLEIGH, M., PIERCE, C.E. and SEED, A., 2004. Sydney 2000 forecast demonstration project: convective storm nowcasting. *Weather and forecasting,* **19**(1), pp. 131-150.

XUE, M., DROEGEMEIER, K.K. and WEBER, D., 2007. Numerical prediction of high-impact local weather: A driver for petascale computing. *Petascale Computing: Algorithms and Applications,* **200**, pp. 103-124.

ZAPPA, M., BEVEN, K.J., BRUEN, M., COFINO, A.S., KOK, K., MARTIN, E., NURMI, P., ORFILA, B., ROULIN, E. and SCHRÖTER, K., 2010. Propagation of uncertainty from observing systems and NWP into hydrological models: COST-731 Working Group 2. *Atmospheric Science Letters,* **11**(2), pp. 83-91.

ZAWADZKI, I., 1973. Statistical properties of precipitation patterns. *Journal of Applied Meteorology,* **12**(3), pp. 459-472.